Multimodal Imaging of Physiologic Changes Induced by Anti-Angiogenic Therapy in Glioblastoma

Olivier Keunen

Dissertation for the degree philosophiae doctor (PhD)

at the University of Bergen

2014

Dissertation date: Dec 18, 2014

ACKNOWLEDGEMENTS

Those who have known me long enough will recognize that I have always wanted to do this. It was clear in my mind, when I was studying engineering in college, that I would one day be applying the techniques I was learning back then to biomedical applications. And among these, tomographic imaging has always been my favorite. That one would be able to 'see' inside the body (or technical speaking build images of underlying tissues based on obscure underlying magnetic properties or the accumulation of some scary radioactive tracers) is still to me truly amazing. I am grateful to have received with this thesis the opportunity to contribute to the fascinating fields of neuroimaging and cancer research.

The work presented here is based on research activities carried out at the Department of Biomedicine of the University of Bergen in Norway, and at the Norlux Neuro-Oncology Laboratory of the Centre de Recherche Public de la Santé in Luxembourg. I would like to express my gratitude to all those who have made this research possible and/or have contributed to it, notably my supervisors, my colleagues, collaborators and my family:

- Prof Frits Thorsen, who accepted to supervise me, knowing I was going to be away most of the time. The advices and encouragements I received at key moments during the thesis have always been highly appreciated, as well as the friendly 'after work' activities!

- Prof Rolf Bjerkvig and Simone Niclou, my other supervisors. You two are the reason I was able to enter this program. Thank you for giving me this opportunity and for believing that a 'computer guy' who knew nothing about tumor biology could become a piece of the puzzle in a successful neuro-oncology research team.

- My estimated colleagues at the Norlux Laboratory: Dr Mikael Johansson, Anais Oudin, Morgane Sanzey, Dr Siti A. Abdul Rahim, Dr Fred Fack, Dr Daniel Stieber, Katja Tiemann, Amandine Bernard, Dr Anna Golebiewska, Dr Sebastien Bougnaud, Virginie Baus, Dr Francisco Azuaje, Dr Sabrina Fritah, Dr Eric van Dyck, Swapnil Bhujbal, Dr Sophie Rodius, Dr Kevin Demeure, Hélène Erasimus, Anne Dirkse, Jill Bohler, Vanessa Barthelemy and Celine Jeanty. Thank you all for welcoming me to the lab, for all the fruitful scientific discussions and for your patience when listening to my 'tech' talks during our lab meetings.

- My collaborators at the University of Bergen and at the Haukeland Hospital in Bergen: Pr Torfinn Taxt, Pr Hrvoje Miletic, Dr Jian Wang, Pr Linda Stuhr, Dr Ingrid Moen, Dr Cecilie Brekke Rygh, Krishna Talasila, Dr Peter Huszthy, Dr Per Sakariassen, Dr Tina Pavlin, Dr Tom Adamsen, Pr Morten Lund-Johansen, Dr Renate Grüner, Nina Obad, Heidi Espedal, Terje Sundstrøm, Ashraf Fathpour, Gerd Salvesen, Ingrid Gavlen, Kai Brandt, Gry Bernes and Aurora Brønstad. What I know about MRI, PET, brain tumors and animal experimentation, I have learned it from the interactions I had with you. Thank you all for your kindness and for making Bergen such a pleasant place to be for me.

- Dr Radovan Jirik and Michal Bartos at the Brno University of Technology, Czech Republic, for introducing me to perfusion imaging and pharmacokinetic modeling.

- Pr Eyal Gottlieb and his collaborators at the Beatson Institute for Cancer Research, UK, for the world-class expertise in metabolomics and the intensive work of processing and analyzing the many samples collected on the project.

- Dr Jean-Claude Schmidt and the CRP Santé Management Team for approving and making this research project possible, and the Ministries of Health and Higher Education and Research of the GD Luxembourg, as well the Fonds National de la Recherche of Luxembourg who financed the research activities and participations to conferences and workshops.

- Siu-Thinh Ho, Birgitte de Martens, Karen Gjertsen and the colleagues at the Technical and administrative services of the CRP Sante, for helping me with the logistics and the administrative work associated with the project and the frequent traveling to Bergen and other parts of the world.

- My parents, family and friends, who are with me day after day. They are my most successful project. Thank you for your kind interest in my professional activities. A very special thanks to Françoise, my wife, for your constant support and encouragements and for organizing everything around me to make this possible, and to my beloved kids Oriane, Isaline, Nathan and Sam, who sometimes needed to deal with a busy traveling father. I hope you'll be as happy in learning and conducting your professional career as I have been doing this PhD project.

ABSTRACT

Glioblastoma (GBM) is the most frequent and malignant form of primary brain tumors. The standard of care for this disease consists in surgical resection, followed by radiotherapy and chemotherapy. Yet, the infiltrative nature of the disease and the resistance to current therapies cause GBMs to inevitably recur, limiting the prognosis to a little more than a year.

GBMs are highly vascularized, and it has long been proposed that interfering with the supply of oxygen and nutrients to the tumor could be used as a therapeutic strategy. Research in this domain has recently lead to the approval in the US of the anti-angiogenic agent bevacizumab for second line treatment of GBMs. An accelerated approval by the Food and Drug Administration was granted on the basis of clinical trials that showed strong radiological response and improved progression free survival in comparison to historical controls. Since then, questions have however been raised about the true antitumor effect of the drug since, despite early improvement in general patient condition, resistance to therapy seems to occur. Benefit in overall survival has not been demonstrated, whether bevacizumab is given as single agent or in combination with chemotherapy.

In the present thesis, multimodal imaging techniques were used to assess the changes induced by anti-angiogenic therapy in a clinically relevant model of GBM. Radiological findings obtained by Magnetic Resonance Imaging (MRI) and Positron Emission Tomography (PET) were compared to histological and molecular analyses to provide insight into the radiological, physiological, metabolic and molecular responses to the bevacizumab therapy.

Using perfusion and diffusion MRI, we observed that anti-angiogenic therapy normalizes the tumor vasculature, and strongly reduces the permeability of blood vessels. While this probably contributes to the improvement in patients condition by reducing peritumoral edema and associated side effects, it also leads to drastic radiological changes which may misleadingly suggest an antitumor effect while the tumor actually continues to grow, possibly adopting a more infiltrative progression pattern. We also found that blood supply to the tumor was strongly reduced after the treatment, an observation of clinical importance that suggests that anti-angiogenic treatment could impair the delivery of systemic chemotherapeutic drugs. The reduced blood supply is also consistent with an increased hypoxia observed in our models when we assessed it by PET. This again has therapeutic significance since increased hypoxia is also associated with reduced efficacy of radiotherapy and chemotherapy.

Metabolic changes induced by anti-angiogenic therapy were evaluated in vivo by Magnetic Resonance Spectroscopy and PET analysis of glucose uptake. These studies highlighted an increased glucose consumption and increased glycolytic metabolism in the treated animals, that was later confirmed by metabolomic analysis of tissue extracts. The putative increased acidification of the tumor microenvironment that may result from this glycolytic activity is a factor that favors the infiltration of tumor cells in the brain parenchyma. This suggests that therapies that combine anti-angiogenic compounds with drugs designed to interfere with the impaired metabolic activity of tumors could be interesting as a new treatment. Preliminary results from preclinical studies that use this strategy seem to support this hypothesis.

We finally examined the hypothesis that anti-angiogenic therapy could impair neuro-cognitive function, a finding that has recently been suggested in a phase III clinical study. In a small preclinical study using measurements of Long Term Potentiation, a technique classically used in neuroscience to determine

memory function, we observed that, in comparison with controls, animals treated with anti-angiogenic therapy showed reduced neuronal plasticity in the hippocampus, a region of the brain associated with spatial learning and short-term memory. These results therefore support the findings of the clinical study but deserve further clinical investigation.

In conclusion, the findings in the present thesis show that MRI and PET have complementary roles in the imaging of brain tumors and can be combined to obtain insight into the mechanisms through which tumor cells adapt to anti-angiogenic therapies. Imaging protocols commonly used in the clinic today provide a partial and sometimes misguiding view of the physiological changes induced by the treatment. The addition of new physiologic and cellular imaging techniques could in the future improve our ability to detect, characterize and treat malignant brain tumors, especially in the context of evolving cellular and molecular therapies.

LIST OF PUBLICATIONS

Paper thesis

This thesis is based on the following papers which are referred to in the text by their Roman numerals

I. **Multimodal imaging of gliomas in the context of evolving cellular and molecular therapies.**
Keunen O, Taxt T, Grüner R, Lund-Johansen M, Tonn JC, Pavlin T, Bjerkvig R, Niclou SP, Thorsen F.
Adv Drug Deliv Rev. 2014 Jul 28. pii: S0169-409X(14)00151-3. doi: 10.1016/j.addr.2014.07.010. [Epub ahead of print] Review.

II. **Anti-VEGF treatment reduces blood supply and increases tumor cell invasion in glioblastoma.**
Keunen O, Johansson M, Oudin A, Sanzey M, Rahim SA, Fack F, Thorsen F, Taxt T, Bartos M, Jirik R, Miletic H, Wang J, Stieber D, Stuhr L, Moen I, Rygh CB, Bjerkvig R, Niclou SP.
Proc Natl Acad Sci U S A. 2011 Mar 1;108(9):3749-54. doi: 10.1073/pnas.1014480108. Epub 2011 Feb 14.

III. **Bevacizumab treatment induces metabolic adaptation towards anaerobic metabolism in glioblastomas.**
Fack F*, Espedal H*, Keunen O*, Golebiewska A, Obad N, Harter P, Mittelbronn M, Bähr O, Weyerbrock A, Miletic H, Sakariassen PØ, Stieber D, Brekke C, Lund-Johansen M, Zheng L, Gottlieb E, Niclou SP, Bjerkvig R.
Acta Neuropathol. 2014, in press.

** Authors contributed equally to this work*

IV. **Bevacizumab treatment for human glioblastoma. Can it induce cognitive impairment?**
Fathpour P, Obad N, Espedal H, Stieber D, Keunen O, Sakariassen PØ, Niclou SP, Bjerkvig R.
Neuro Oncol. 2014 May;16(5):754-6. doi: 10.1093/neuonc/nou013.

Impact and recognition

Paper II has been cited more than 150 times in peer-reviewed journals at the time of preparing this thesis (source Thomson Reuters Web of Science).

The work published in Papers II and III was presented at international conferences and was awarded the following prizes:

- Physiological & Biological Response of Anti-Angiogenic Therapy in a Glioblastoma Model Using Multi-Modal MRI & Molecular Analysis - ISMRM Workshop 'Improving cancer treatment with advanced MR', Santa Cruz, CA, USA - Sept 2010 - William Negendank Award (Second Prize)
- Mechanism of action of anti-angiogenic therapy in malignant gliomas assessed by multi-modal imaging - MedViz PhD national conference on medical imaging, Bergen, Norway, Jan 2011 - Best Presentation Award (Second Prize)
- Metabolic changes induced by anti-angiogenic therapy in Glioblastoma - ISMRM Workshop 'Magnetic resonance of Cancer Gone Multimodal', Valencia, Spain, Feb 2013 - William Negendank Award (Third Prize)

Other collaborations

In addition to the work that resulted in the papers presented in this thesis, a number of collaborations were established during the course of the PhD project that lead to co-authorships on the following papers:

V. **Perfusion analysis of dynamic contrast enhanced magnetic resonance images using a fully continuous tissue homogeneity model with mean transit**.
M Bartos, O Keunen, R Jirik, R Bjerkvig, T Taxt.
Anal Biomed Sign Images 20, 269-274.

In this conference paper, issues related to the estimation of perfusion parameters using pharmacokinetic models based on MRI data are discussed. Practical solutions to common convergence problems are presented and applied to perfusion studies in an animal model.

VI. **EGFR wild-type amplification and activation promote invasion and development of glioblastoma independent of angiogenesis.**
Talasila KM, Soentgerath A, Euskirchen P, Rosland GV, Wang J, Huszthy PC, Prestegarden L, Skaftnesmo KO, Sakariassen PØ, Eskilsson E, Stieber D, Keunen O, Brekka N, Moen I, Nigro JM, Vintermyr OK, Lund-Johansen M, Niclou S, Mørk SJ, Enger PO, Bjerkvig R, Miletic H.
Acta Neuropathol. 2013 May;125(5):683-98.

This paper describes the role of EGFR, a cell surface receptor often overexpressed in GBM, in non-angiogenic, invasive tumor growth. MRI was used to assess the perfusion and infiltration characteristics of animal models in which EGFR was over- or under- expressed, and to evaluate the changes induced by a treatment inhibiting EGFR activity.

VII. **The soluble form of the tumor suppressor Lrig1 potently inhibits in vivo glioma growth irrespective of EGF receptor status.**
Johansson M, Oudin A, Tiemann K, Bernard A, Golebiewska A, Keunen O, Fack F, Stieber D, Wang B, Hedman H, Niclou SP.
Neuro Oncol. 2013 Sep;15(9):1200-11.

This paper focuses on the therapeutic potential in GBM treatment of LRIG1, a protein that interacts with receptor tyrosine kinases of the EGFR family. In vitro and in vivo studies were conducted, using intracranially implanted encapsulated cells for the local delivery of LRIG1. MRI was used to evaluate and quantify the effect of the therapy on tumor growth.

VIII. **Molecular interactions between tumor and stromal cells in a clinically relevant mouse model of glioblastoma.**
S Bougnaud, A Golebiewska, D Stieber, A Oudin, O Keunen, A Bernard, F Azuaje, T Kaoma, PV Nazarov, L Vallar, NHC. Brons, P Harter, M Mittelbronn, A Mock, C Herold-Mende, T Sundstrøm, H Miletic, R Bjerkvig, and SP Niclou.
Manuscript in preparation.

This manuscript addresses the role of the micro-environment in tumor development of patient-derived xenografts. Different phenotypes going from invasive to angiogenic and mixed models have been established and are characterized by histology, molecular analysis and MRI.

IX. **Epigenetic activity of PPARγ agonists increases the anticancer effect of HDACi on multiple myeloma cells.**
N Aouali, A Broukou, M Bosseler, O Keunen, V Schlesser, B Janji, V Palissot, P Stordeur and G Berchem.
Manuscript submitted to British Journal of Haematology.

In this manuscript, the authors report the promising results of combining, in an animal model of multiple myeloma, histone deacetylase inhibitors, that regulate the conformation of chromatin and gene expression, with peroxisome proliferator-activated receptor gamma agonists, expressed during adipogenesis and involved in cell cycle arrest, apoptosis and inhibition of cancer development.

These collaborative papers are not further discussed within this thesis.

Contributions

The contributions to the different papers is summarized in the following table

Papers >	I	II	III	IV	V	VI	VII	VIII	IX
Study design	√	√	√						
Experimental work	[1]	√	√	√	√		√	√	
Data analysis	[1]	√	√	√		√			√
Manuscript redaction	√	√	√						

Table 1 – Contributions to the papers

[1] Paper I is a review paper with no experimental work nor data analysis

ABBREVIATIONS

ADC	Apparent Diffusion Coefficient
APT	Amide Proton Transfer
ASL	Arterial Spin Labeling
BOLD	Blood Oxygen Level Dependent
CEST	Chemical Exchange Saturation Transfer
CSC	Cancer Stem Cell or Cancer Stem-like Cells
CSI	Chemical Shift Imaging
CT	Computerized Tomography
DCE	Dynamic Contrast Enhanced
DSC	Dynamic Susceptibility Contrast
DTI	Diffusion Tensor Imaging
DWI	Diffusion Weighted Imaging
EGFR	Epidermal Growth Factor Receptor
FDA	Federal Drug Agency
FDG	Fluorodeoxyglucose
FLAIR	Fluid Attenuated Inversion Recovery
FMISO	Fluoromisonidazole
fMRI	Functional Magnetic Resonance Imaging
GBM	Glioblastoma Multiforme
Gd	Gadolinium
HIF	Hypoxia Inducible Factor
IDH	Isocitrate Dehydrogenase
IHC	Immuno Histo Chemistry
MRI	Magnetic Resonance Imaging
MRS	Magnetic Resonance Spectroscopy
MT	Magnetization Transfer
NMR	Nuclear Magnetic Resonance
PARA-CEST	Paramagnetic Chemical Exchange Saturation Transfer

PET	Positron Emission Tomography
PWI	Perfusion Weighted Imaging
rCBV	Relative Cerebral Blood Volume
SPECT	Single Photon Emission Computed Tomography
SPIO	Superparamagnetic Iron Oxyde
SWI	Susceptibility Weighted Imaging
TKI	Tyrosine Kinase Inhibitors
TMZ	Temozolomide
TOF-MRA	Time Of Flight - Magnetic Resonance Angiography
US	Ultrasound
USPIO	Ultrasmall Superparamagnetic Iron Oxyde
UTE	Ultrashort Echo Time
VEGFR	Vascular Endothelial Growth Factor Receptor

1 INTRODUCTION

1.1 Gliomas

Gliomas are brain tumors that result from an uncontrolled proliferation of glial cells, the cells that provide support and protective functions to the neurons. Unlike neurons, glial cells in the human brain have the ability to divide and multiply, and the deregulation of these processes gives rise to this type of tumor.

Other types of brain tumors include meningioma, lymphoma, tumors of the cranial and paraspinal nerves, as well as secondary tumors, which represent brain metastases derived from non-cranial tumor cells that home to the brain.

1.1.1 Classification and grading

The most commonly used scheme for the classification and grading of brain tumors is the one defined by the World Health Organization (WHO) [1]. In this scheme, glial tumors are classified according to their location and their putative glial cell lineage. Astrocytomas, the most common glial tumors, are believed to develop from cells of the astrocytic lineage. These cells of neuroepithelial origin provide nutrients to the neurons and biochemical support to endothelial cells. They represent an important component of the blood-brain-barrier. Other types of gliomas include oligodendroglioma, ependymoma, brain stem glioma and mixed gliomas.

The histopathological features of the gliomas are commonly used to define their grade and characterize their aggressiveness:

- Grade I tumors have a low proliferative potential with no infiltrative compartment and may be totally resected by surgery.
- Grade II tumors are infiltrative and low in mitotic activity but recur and tend to progress to higher grades of malignancy.
- Grade III tumors display high mitotic activity, increased cellularity, nuclear polymorphism, clear infiltrative capability and anaplasia.
- Grade IV tumors (glioblastomas), in addition, display microvascular proliferation and pseudopallisading necrosis.

Histological grading is highly relevant to predict the patient's prognosis and to select treatment options. Low grade gliomas (I and II) are considered benign tumors, while high grade gliomas (III and IV) are malignant and carry a worse prognosis.

1.1.2 Incidence and prognosis

Glioblastoma (GBM) is the most frequent of brain tumors, accounting for approximately 12-15% of all intracranial neoplasms. Its incidence is about 3-4 new cases per year and per 100,000 inhabitants in most North American and European countries [1]. GBMs can develop from lower grade diffuse astrocytoma or anaplastic astrocytoma and are then termed secondary GBMs. More commonly though, in approximately 95% of the cases, they manifest rapidly without recognizable signs of a preceding precursor lesion and are then called primary GBMs [2].

Tumor grade, radial tumor resection, younger age, good performance status and intact neurological function are favorable prognostic factors in high grade gliomas [3]. Yet, they are most of the time

incurable, and the high mortality rate thus turns these rather infrequent tumors into an important cause of cancer-related death [4, 5].

The current standard of care for newly diagnosed GBMs extends survival to about 14 months [6]. This is only achieved through aggressive treatment including surgery, radiation therapy and chemotherapy, leaving most of the patients in a poor condition. Less than 10% of the patients survive more than 5 years [7].

1.1.3 Conventional therapies

1.1.3.1 Surgical resection

Once a preliminary diagnosis is established on the basis of clinical history and radiographic findings, the first step is typically tumor removal by neurosurgery, provided that a suitable safe surgical route is possible.

This surgical step is critical for the reduction of elevated intracranial pressure and management of seizures. The neurosurgeon also collects the tissue material that the neuropathologist uses to determine the diagnosis that establishes tumor grade and defines the next steps in patient care.

1.1.3.2 Radio-chemotherapy

Surgical resection is often followed by fractionated external beam radiation therapy and chemotherapy using the DNA-alkylating agent Temozolomide. Dosage and schedule of delivery are based on the protocol developed by Stupp et al. in their landmark clinical trial in 2005 [6].

The methylation status of the methyl-guanine methyl transferase (MGMT) gene promoter influences the tumor's ability to repair DNA damages and thus appears to be a predictive factor for response to chemotherapy with Temozolomide [8]. Yet, determination of the MGMT status doesn't influence clinical decision-making at the moment, in the absence of alternative treatment.

1.1.3.3 Treatment at recurrence

No established therapy with survival benefit is available at recurrence. Single agents, such as the DNA alkylating agents carmustine or lomustine, may achieve some tumor control in selected patients. Also, re-operation and the use of chemotherapy-impregnated polymers following repeated surgery, only provide marginal survival benefits in selected patients [3].

1.1.4 Challenges associated with the treatment of GBMs

GBMs have a number of inherent features that make their treatment with conventional therapies challenging.

1.1.4.1 Heterogeneity

GBMs are among the most heterogeneous tumors. Tumors from patients can vary by their gene mutations, epigenetic and phenotypic profiles. Furthermore, within GBMs, cells with different genotypes may co-exist in a microenvironment made up of varying stromal and immunocompetent cells and extracellular matrix components. This heterogeneity represents a challenge for the characterization and treatment of the pathological tissue, and contributes to drug resistance and tumor recurrence [9].

1.1.4.2 Invasiveness

GBMs are invasive in nature and the infiltration of tumor cells in the brain parenchyma also represents a challenge for their management. First, it makes complete resection by surgery practically impossible, leaving the patient with residual tumor cells that are believed to be the cause of tumor relapse. In addition, low concentrations of tumor cells in the infiltrative compartment are difficult to detect by current imaging methods, making the planning of radiotherapy challenging. Finally, the invasive tumor cells are frequently present in brain areas where there is an intact blood-brain barrier, making drug delivery to these cells difficult.

1.1.4.3 Aberrant tumor vasculature

For the tumor to grow beyond the size of a few cubic millimeters, it needs to engage in a process called angiogenesis by which new vessels are formed from the existing vasculature. This 'angiogenic switch' is necessary for tumor cells to keep receiving the oxygen and nutrients they need to sustain their growth. The new vessels formed are, however, growing in an anarchic way and lack the maturity of normal blood vessels [10]. This has a number of consequences: First of all, the blood-brain-barrier of the tumor vessels is impaired which causes fluid from the blood to leak out to brain tissue causing edema and associated swelling. This phenomenon is responsible for many of the symptoms observed in brain tumor patients. Then, tumor cells that go through cycles of well and poor oxygenation stages adapt to these changing conditions. They are able to survive under hypoxic conditions by switching to a dormant mode, thereby escaping radio- and chemo- therapy treatments, which typically target proliferating cells.

1.1.4.4 Treatment specificity

Radiotherapy uses ionizing radiation to kill tumor cells but it also affects surrounding tissue. Chemotherapy with alkylating agents affects dividing cells, among which tumor cells, by interfering with cellular DNA replication mechanisms. The ideal treatment would be one that can specifically target the tumor cells without affecting the normal healthy surrounding cells. Different approaches for such targeted therapies are under development, including small molecules that interfere with the signaling events associated with glioma growth, immunotherapies, gene and viral therapies, and strategies for the local delivery of therapeutic compounds. Recent developments related to these therapies have been reviewed in a recent special issue of 'The Cancer Journal' [11] and were summarized in Paper I.

1.2 Anti-angiogenic therapy

Among the most promising new therapies are those that target the abnormal proliferation of endothelial cells that support tumor growth. Such inhibitors of angiogenesis are attractive for the treatment of the highly vascularized GBMs. The mechanisms of action of anti-angiogenic drugs was initially expected to be the prevention of new blood vessel formation and pruning of existing tumor vessels, leading to the deprivation of nutrients and oxygen supply to the tumor [12]. Since their introduction however, additional mechanisms of actions of these drugs have been proposed, such as a vascular normalization with possible improved tumor perfusion and delivery of cytotoxic drugs [13], and the disruption of the perivascular cancer stem cell niche [14].

1.2.1 Anti-angiogenic compounds

The VEGF pathway, which is the main driver of angiogenesis [15], has been the main target of several inhibitors in clinical development. VEGF-A is secreted by tumor cells and binds to the receptor VEGFR-2 at

the surface of endothelial cells. This activates downstream signaling pathways resulting in increased vascular permeability, endothelial cell migration and recruitment of endothelial precursor cells [16]. Clinical developments have led to the approval in 2009 by the FDA of Bevacizumab, a monoclonal antibody against VEGF-A, for the second line treatment of GBMs. An accelerated approval was granted following two phase II clinical studies that showed impressive radiological responses and an improved rate of six months progression free survival (PFS) in comparison with historical data [17, 18]. Addition of the chemotherapeutic agent irinotecan did not sufficiently improve PFS in regard to the additional toxicity induced [17].

Another category of anti-angiogenic agents comprises the small molecule tyrosine kinase inhibitors (TKI) that target several proangiogenic molecules. The most studied TKI in GBM, cediranib, blocks all VEGFRs, c.kit and PDGFR α/β. Its use in clinical trials, either alone or in combination with the chemotherapeutic agent lomustine has provided limited benefits so far [19, 20]. One concern with these TKI's is the increased toxicity due to off target effects compared to antibody based therapeutic strategies.

1.2.2 Response to anti-angiogenic therapy and adaptation mechanisms

Bevacizumab provides evident benefits of improved quality of life in a number of patients that respond to the treatment. This most likely results from the reduction in blood vessel permeability and associated vasogenic edema [21], that makes it possible to reduce or eliminate the chronic use of corticosteroids and its related toxicities (osteoporosis, weight gain, insomnia, infection and psychiatric effects). Bevacizumab also seems to be beneficial for radiation induced necrosis [22], since damaged endothelial cells also come with an important release of VEGF and progressive vasogenic edema.

Despite these benefits, concerns have been expressed about a real anti-tumor effect of the drug. All patients eventually relapse and the overall survival is not improved [23, 24]. Several evasive/adaptive resistance mechanisms may be induced, including up-regulation of alternative proangiogenic pathways, improved protection of the tumor neovasculature by increased pericyte coverage, and an increased invasiveness of tumor cells that co-opt native brain blood vessels [25, 26]. Several clinical trials have been initiated that combine Bevacizumab with radiochemotherapy, but results so far have failed to demonstrated significant benefit in overall survival [27, 28].

Toxicities associated with anti-angiogenic therapies are typically rare but potentially serious. They include hypertension, intratumoral hemorrhage, thromboembolic events, poor wound healing, bowel perforation, proteinuria, kidney damage, fatigue and diarrhea [29, 30].

1.3 Modalities for the imaging of brain tumors

Neuroimaging has, over the years, become invaluable for the management of gliomas. It is used for the detection and localization of tumors, for the planning of neurosurgery and radiotherapy and to assess treatment efficacy [31].

Magnetic Resonance Imaging (MRI), an imaging modality that builds 3D tomographic images of soft tissues based on the magnetic properties of hydrogen nuclei, is often the preferred modality, owing to the variety of contrasts available, and its ability to provide morphological, physiological and metabolic information about the tumor [32]. Positron Emission Tomography (PET), a nuclear imaging modality that uses the labeling of endogenous molecules by positron emitting radionuclides to follow their distribution and accumulation in the body, can complement MRI nicely by providing access to molecular targets with

very high sensitivity. Tracers of proliferation and metabolic activity are for example increasingly being used in pre-therapy assessment and in the monitoring of treatment response [33].

Other less frequently used modalities include Computerized tomography (CT), a modality that creates 3D images based on the attenuation of x-rays in tissue, which can be used to provide the anatomical context in a PET study, but also to detect tumors or assess physiological parameters in perfusion studies [34]. Single Photon Emission Computed Tomography (SPECT), another nuclear imaging technique with radiotracers that are easier and cheaper to produce than those used for PET, can be used to assess proliferation [35]. And Ultrasound, a technique based on the reflection of sound waves, is used in specialized applications such as pediatric brain tumors [36] and tumor delineation during surgery [37].

The use of these imaging modalities in clinical and preclinical settings, especially in the context of molecular and cellular therapies, has extensively been reviewed in Paper I. The rest of the present chapter summarizes the most common neuroimaging protocols that are used in the clinic today, as well as some of their limitations in the context of brain tumor imaging.

1.3.1 MRI

MRI anatomical sequences are used to localize tumors and possibly associated peritumoral edema, hemorrhages or necrosis. Physiological sequences provide access to parameters related to tumor perfusion, angiogenesis and cellularity, that have prognostic potential and can be used to assess response to therapy [38, 39]. Spectroscopy series can assist in characterizing tumors and to distinguish them from other malignancies [40, 41] .

Fig 1, reproduced from Paper I, illustrates the use of common MRI protocols for a GBM patient.

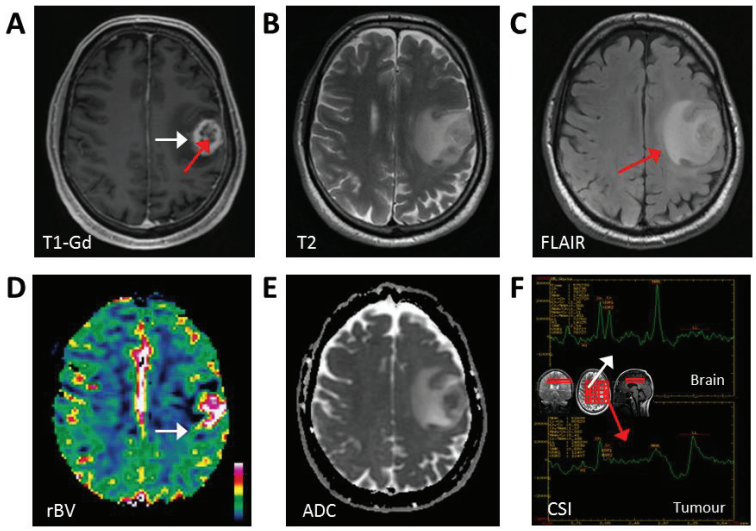

Fig 1 – Multiparametric assessment of brain tumors with MRI

Multiparametric MRI provides morphological, physiological and metabolic data on the tumor. In the present case, for a patient diagnosed with GBM: (A) A T1 sequence after injection of Gd contrast shows a necrotic

tumor core (red arrow) surrounded by a hyperintense ring of contrast enhancement (white arrow) caused by a leaky tumor vasculature. (B) T2 sequence showing a large abnormal signal with a hyperintense core. (C) The T2-FLAIR sequence, a T2-like sequence in which the high signal produced by CSF is removed, provides insight into the extent of the edema (red arrow). (D) The rCBV map shows active tumor cells at the periphery of the tumor (white arrow). (E) The ADC map shows area of abnormal water molecules diffusion which may be caused by a combination of factors including necrosis, edema and hypercellularity. (F) CSI spectroscopy showing, for the given grid position, spectra corresponding to voxels of healthy brain (white arrow) and tumor tissue (red arrows). Gd: Gadolinium, ADC: Apparent Diffusion Coefficient, rCBV: relative Cerebral Blood Volume, FLAIR: Fluid Attenuated Inversion Recovery, CSF: Cerebro Spinal Fluid, CSI: Chemical Shift Imaging.

1.3.2 PET

PET tracers based on amino acid metabolism or nucleic acids are used to assess proliferation and metabolic activity, and to predict and evaluate response to treatment [42]. Tracers also exist for the assessment of molecular mechanisms associated with cellular death [43], changes in micro-environment [44] or drug delivery [45] .

Fig 2, reproduced from Paper I, illustrates PET protocols commonly used in the clinic.

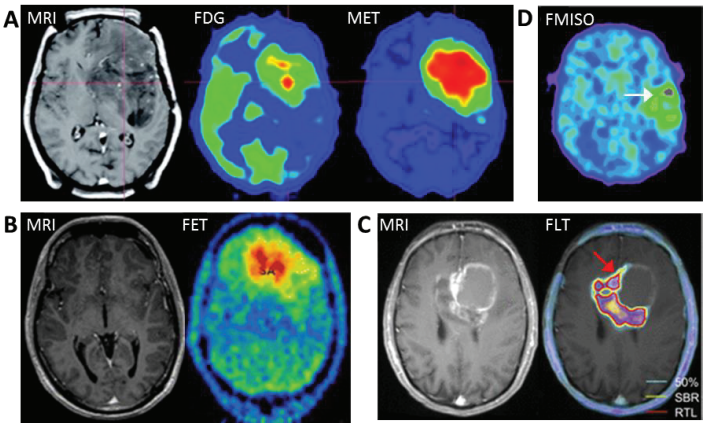

Fig 2 – Molecular imaging of brain tumors with PET

Typical PET tracers used for molecular imaging of gliomas in the clinic: (A) Metabolic imaging of an infiltrating anaplastic astrocytoma patient. Uptake of ^{18}F-FDG is higher in the tumor than in the surrounding gray matter. Uptake of ^{11}C-MET is also higher in the tumor and extends beyond the area of high FDG uptake. (B) ^{18}FET-PET of a second glioma patient treated with antiangiogenic therapy, showing high tracer uptake despite the absence of contrast enhancement in MRI. (C) ^{18}F-FLT overlaid to MRI for a third GBM patient, showing high uptake values indicative of high tumor cell proliferation in the tumor compartment infiltrating through the corpus callosum (red arrow). (D) ^{18}F-FMISO scan of a fourth patient with a GBM in the left temporal lobe, showing the accumulation of the tracer in hypoxic regions of the tumor (white arrow). Information in panels A, B, C, D reproduced and adapted with authorization from [46-49] respectively, © by the Society of Nuclear Medicine And Molecular Imaging, Inc. ^{18}F-FDG: ^{18}F-Fluorodeoxyglucose, ^{11}C-MET: ^{11}C-methionine, ^{18}FET: ^{18}F-fluor-ethyl-tyrosine, ^{18}F-FLT: ^{18}F-Fluorothymidine, ^{18}F-FMISO: ^{18}F-Fluoromisonidazole.

1.3.3 Limitations of current imaging approaches

The criteria that are most commonly used in clinical settings to assess treatment efficiency (Mac Donalds/WHO) were established in 1990 [50]. Response to therapy is based on changes in tumor volume measured from the 2D sections displaying the largest tumor in CT or T1c scans after contrast injection, taken 4 weeks apart.

Conventional imaging based on T1-weighted sequence acquired after the injection of Gadolinium-based contrast agents, can however suffer from several problems:

Pseudo-progression

An increase in contrast enhancement can occur shortly after chemoradiation, induced by inflammation or, many months after, by radiation necrosis. This enhancement is not a reflection of tumor progression, and has therefore been termed 'pseudo-progression' [51]. Given the inability of T1c to distinguish between pseudo-progression and early tumor recurrence, a number of alternative approaches have been proposed: A low Apparent Diffusion Coefficient (ADC) obtained from Diffusion Weighted Imaging (DWI) sequences can be indicative of early recurrence [52], as would also a high relative blood flow obtained from PWI [39]. PET tracers of amino acid metabolism such as ^{11}C-methionine [53, 54], ^{18}F-ethyl-tyrosine [55] have also been proposed. These methods may however suffer from a lack of sensitivity and specificity in distinguishing tumor recurrence from inflammation, such that confirmation from tissue biopsies remains the standard method.

Pseudo-response

Pseudo-response is a reduction of contrast uptake in T1-weighted MRI, such as after anti-angiogenic therapy for example, despite continued tumor progression, that can sometimes be evidenced by T2-weighted or FLAIR protocols, by MRS or by PET protocols using tracers based on amino acid metabolism or nucleic acids [56].

Tumor infiltration

The infiltrative compartment of GBMs is difficult to visualize in MRI, whose sensitivity is limited to about 10^{-3} to 10^{-5} mole/liter. The standard protocols used in the clinic are also non-specific. Tumor cells cannot readily be distinguished from normal brain cells, and can only be investigated through indirect parameters such as longitudinal (T1) and transversal (T2) relaxation. Experimental protocols are being developed to address these issues. Paper I describes some of these protocols, among which Amide Proton Transfer, Restricted Spectrum Imaging and nanoparticles seemed to be the most promising candidates. To visualize the zone infiltrated with few tumor cells, PET, with its high sensitivity (10^{-11}-10^{-12} mole/liter), appears to remain the most interesting modality though, provided that the tracers can effectively reach the tumor cells through a possibly intact blood-brain-barrier.

The difficulties in assessing the response to therapy have prompted a panel of experts, the RANO group, to recently update the proposed criteria [57]. The new recommendations distinguish contrast enhancement within and outside the area of radiation, and introduce FLAIR to assess the infiltrative component of brain tumors, although without formal directions on how to use it for quantitative assessment of tumor progression.

1.4 Preclinical models of GBM

The choice of animal models is key to ensure that pre-clinical findings are relevant for the clinic. In this respect, a good animal model needs to reflect the biological properties of the patient tumor, the heterogeneity of its subpopulations, and the complex interplay between tumor and host components including anatomical barriers, extracellular matrix molecules, cytokines/growth factors and populations of endothelial and immune response cells [58].

Chemically induced syngenic models and xenogenic glioma models established as cell lines differ from human glioma biopsy material at the molecular level because of a genetic drift and clonal selection acquired when passaging cells in vitro. This typically results in the loss of important histological features such as single cell infiltration, microvascular abnormalities and necrosis that are characteristic of GBM [59].

The model used in the present studies is the biopsy spheroid xenograft model described previously [60]. Briefly, patient tumor biopsies are minced and short term cultured until they form multicellular aggregates. These so-called spheroids, which maintain the tissue architecture of the biopsy including endothelial cells, extracellular matrix components and resident macrophages, are then implanted into the brains of immunodeficient athymic rats. After passaging and adaptation to the host environment, the established xenograft tumors display the histological features of human GBMs, including infiltrative growth, angiogenesis and necrosis, while maintaining the heterogeneity of tumor subpopulations and the genetic mutations of the primary tumor [60, 61] .

Fig 3, reproduced from the supplementary information of Paper II, illustrates how the histologic and genetic features of the primary tumor are retained in the xenograft for the model P3 used in the studies.

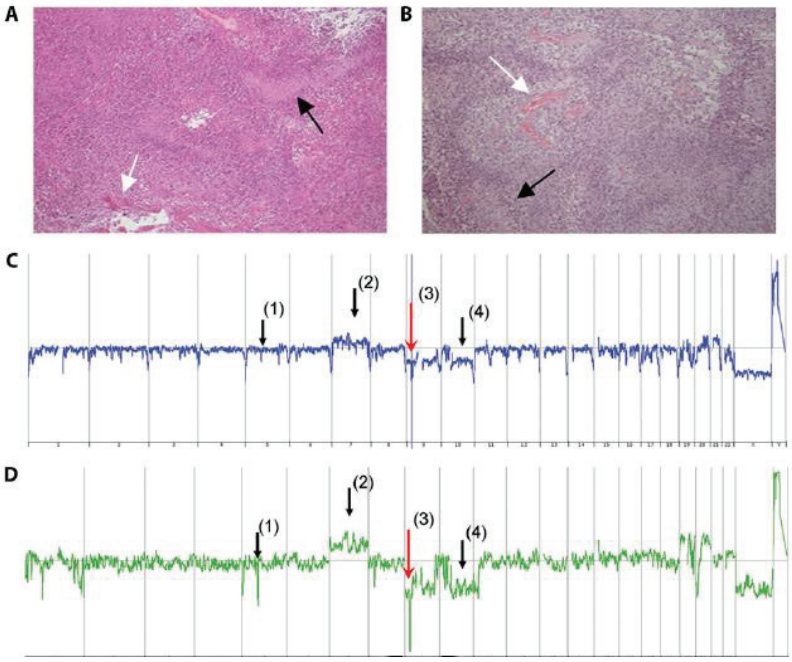

Fig 3 – Histology and genetic profile of primary GBM and corresponding xenograft

(A-B) hematoxylin/eosin stained sections of the primary tumor (A) and rat xenograft (B). Both sections show palisading necrosis (black arrow) and vascular proliferation (white arrow), which are histological features of GBM. (C-D) Genetic profiles of the primary tumor and corresponding xenografts. Array comparative genomic hybridization was used to determine the relative chromosome copy numbers. Similar chromosomal aberrations, that are typical of GBMs [47], can be observed in both the primary tumor (C) and the xenograft (D): (1) deletion of the PIK3R1 gene on chromosome 5; (2) amplification of chromosome 7 including EGFR; (3) deletion of CDKN2A/B and loss of one copy of chromosome 9; and (4) deletion of chromosome 10 including the PTEN gene.

2 AIMS OF THE THESIS

The anti-angiogenic agent bevacizumab has not provided the true clinical benefit that patients and physicians hoped for when the FDA approved it for second line treatment of GBM in May 2009. Despite the sometimes drastic radiological changes observed in many patients that responded well to this therapy, often associated with an improvement of patient's general condition, adaptation mechanisms take place and no significant gain in overall survival is achieved whether bevacizumab is used as first or second line treatment, alone or in combination with chemotherapy [17, 18, 23, 24].

The purpose of this thesis was therefore to explore whether neuroimaging modalities could be used to improve our understanding of the adaptation mechanisms that take place following anti-angiogenic therapies, and evaluate whether the imaging protocols that are currently used in the clinic are sufficient to provide a reliable assessment of the tumor evolution in the context of such therapies.

Specifically we:

1. Investigated the biological, physiological and metabolic changes induced by anti-angiogenic therapy in a clinically relevant model of GBM.
2. Evaluated how MRI and PET protocols, currently used in the clinic or experimental settings, can be used to evaluate responses to anti-angiogenic therapies.
3. Provided the rationale from which to develop new treatment strategies that combine anti-angiogenic agents with agents that interfere with the mechanisms of resistance to this type of therapy.

3 SUMMARY OF PAPERS

3.1 Materials and Methods

3.1.1 Animal studies design

During the course of the thesis, 5 main studies involving a total of 112 animals were conducted. All studies followed a similar setup that is summarized in Fig 4, and detailed in the Materials and Methods sections of Papers II and III.

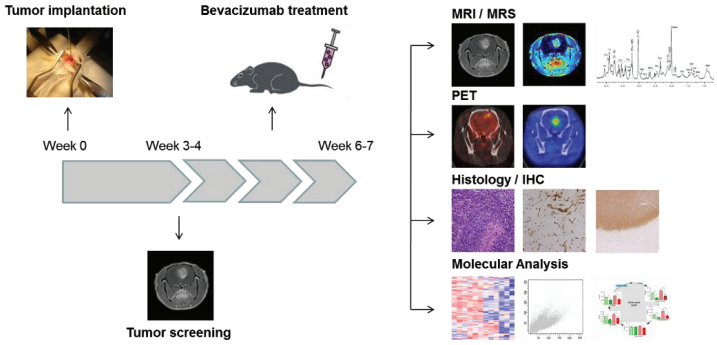

Fig 4 – Generic animal studies setup

GBM-derived spheroids from 2 patients (P3 and P13) were expanded through serial transplantation in nude rats. Tumors were implanted intracranially on day 1. After 3 to 4 weeks (depending on the growth pattern of the GBM model used), a MRI screening session was performed to verify tumor take and randomly assign animals to treatment groups. Animals were treated with bevacizumab or saline for 3 weeks or until neurological symptoms occurred. At the end of the treatment period, extensive imaging was performed, animals were sacrificed and tissue was harvested for histology and/or molecular analysis. MRI: Magnetic Resonance Imaging, MRS: Magnetic Resonance Spectroscopy, PET: Positron Emission Tomography, IHC: ImmunoHistoChemistry

The purpose of the individual studies was the following:

- Study 1 : Assess radiological and physiological changes induced by anti-angiogenic therapy
- Study 2 : Characterize metabolic response to anti-angiogenic therapy using metabolomics
- Study 3 : Assess changes induced by anti-angiogenic therapy in healthy animals
- Study 4 : Examine the dynamic of vascular changes following anti-angiogenic therapy
- Study 5 : Validate findings of metabolomics study by in vivo metabolic imaging

Table 2 summarizes the type of analysis that was performed in each of these studies

Study	Short description	Rats	Model(s) used	MRI	MRS	PET	Hist	RNA	Prot	Met	Reported in
1	Physiology	38	P3	√	√		√	√	√		Paper II
2	Metabolomics	28	P3	√	√		√	√		√	Paper III
3	Healthy animals	8	-	√	√		√	√		√	Paper IV
4	Vascular normalization	26	P3, P13	√	√	√	√	√	√		n.p.
5	Metabolic imaging	12	P3, P13	√		√	√				Paper III

Table 2 – Summary of animal studies

MRI: Magnetic Resonance Imaging, MRS: Magnetic Resonance Spectroscopy, PET: Positron Emission Tomography, Hist: Histological/Immunohistochemical analysis, RNA: RiboNucleic Acid (for gene expression analysis), Prot.: Proteins analysis, Met.: Metabolites analysis, n.p: Data not published (manuscript in preparation)

All animal studies were conducted in the Laboratory and Animal Facility of the University of Bergen (UiB) with approval of the local ethical committee. MRI and PET acquisitions were performed on the 7T Bruker Pharmascan and Mediso Nanoscan PET/CT imagers available at the Molecular Imaging Center, Department of Biomedicine, University of Bergen, Norway.

3.1.2 MRI/PET protocols

MRI was used to provide in vivo anatomical, physiological and metabolic information about the tumor and its vascular supply. The protocols used are detailed in the Materials and Methods sections of Paper II and III and summarized and illustrated hereafter:

Anatomy

T2-weighted series were used to obtain anatomical views of rat brains. Tumors typically have prolonged T2 relaxation times and appear hyperintense relative to normal brain in these sequences. However edema, large vessels, hemorrhage, necrosis and calcification all have different T2 and contribute to the heterogeneity of the signal observed.

T1-weighted series were used to highlight the presence of tumors after the injection of Gadolinium-based contrast agents. Tumor vessels have a disrupted blood-brain barrier, allowing the contrast agent to leak out and accumulate in the extracellular space of the tumor tissue. As a result, the tumor becomes brighter than surrounding tissue due to the shortening of the T1 relaxation time. Contrast enhancement was consistently used to verify the angiogenic phenotype of the xenografted tumors.

FLAIR sequences are similar to T2-weighted (or T1-weighted) acquisitions, except that the signal of the cerebrospinal fluid is removed. They can be used to delineate the boundaries of tumors in the vicinity of ventricles and to evaluate peritumoral edema and tumor infiltration.

Fig 5 illustrates the use of the T1, T2 and T2-FLAIR sequences in a xenografted animal.

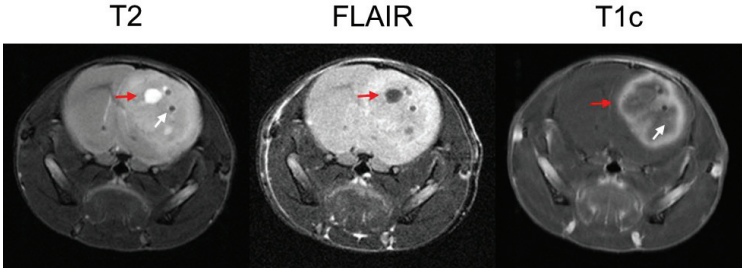

Fig 5 –MRI anatomical images for a mouse implanted with the GBM model P13

T2-weighted MRI (left panel) shows a large heterogeneous tumor in the right hemisphere expanding to the left, with dark spots (white arrow) that possibly correspond to angiogenic blood vessels and white spots (red arrow) that reflect fluid accumulation. The T2-FLAIR MRI (center panel) suggests the central white spot in the T2-weighted series (red arrow) to contain CSF. T1-weighted MRI (right panel) after injection of Gd-based contrast agent reveals a ring of contrast enhancement (red arrow), associated with leaky vasculature, surrounding a central necrotic region (white arrow), in a pattern similar to those observed in clinical GBMs. FLAIR: Fluid Attenuated Inversion Recovery, CSF: Cerebrospinal Fluid, Gd: Gadolinium

Physiology

Dynamic contrast enhanced (DCE) MRI was used to assess perfusion parameters. The sequence requires the bolus injection of a contrast agent followed by the rapid acquisition of T1-weighted sequences over time. The dynamics of contrast agent concentration curves obtained are used in pharmacokinetic models to derive key physiological parameters such as blood volume, blood flow, transit time, interstitial space volume fraction as well as blood vessel permeability parameters. These perfusion parameters are important in order to delineate the physiological changes that occur during tumor development or in response to therapy.

Dynamic susceptibility contrast (DSC) MRI, is an alternative perfusion method based on T2 or T2* weighted rapid sequences acquired at the first passage of a bolus of contrast agent. Arterial Spin Labeling (ASL), is yet another perfusion analysis method based on the labeling of water molecules in the blood without the need of an exogenous contrast agent. All three perfusion methods were used in the vascular normalization study, for a methodological comparison. Results are not reported here, but will be published separately. In the present work, DCE was the preferred method because it provides access to blood vessel permeability parameters in addition to the blood flow and blood volume parameters provided by the other methods.

Diffusion Weighted Imaging (DWI) was used to analyze the diffusion of water molecules in tissue. The presence of membranes restricts this diffusion causing hypercellular regions to appear hypointense on DWI images. However, other factors such as the presence of edema or necrosis facilitate diffusion and can be confounding factors when assessing tumor regions.

Fig 6 illustrates the use of perfusion and diffusion MRI to assess physiological parameters of the tumor.

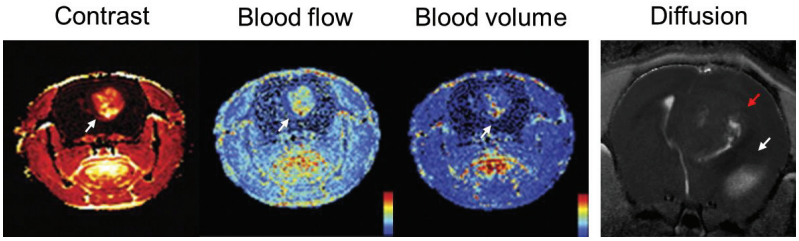

Fig 6 – Examples of MRI perfusion and diffusion parameters

Left panel: AUC map showing contrast accumulation (white arrow) after injection of Gd-based contrast agent, for a rat implanted with a GBM in the right hemisphere. Middle left and middle right panel: Blood flow and blood volume maps obtained by DCE-MRI perfusion analysis, showing area of elevated blood flow and corresponding blood volume (white arrows) in a region of the tumor associated with highly proliferating cells. Right panel: ADC map showing area of heterogeneous water molecules diffusion corresponding to the tumor (red arrow) and of elevated diffusion corresponding to the presence of CSF in a ventricle (white arrow). AUC: Area Under the Curve, Gd: Gadolinium, DCE-MRI: Dynamic Contrast Enhanced – Magnetic Resonance Imaging, ADC: Apparent Diffusion Coefficient

Metabolism

Single voxel spectroscopy was used to quantify the concentrations of a small number of abundant metabolites in vivo. For example, N-acetylaspartate, a marker of neuronal function is elevated in healthy tissue and reduced in tumor. Choline, a component of the cellular membrane is elevated in the proliferating cells of tumors. Lactate is also often elevated in tumors that use glycolysis for energy production.

Fig 7 illustrates the use of MRS to assess and quantify the presence of abundant metabolites in the tumor.

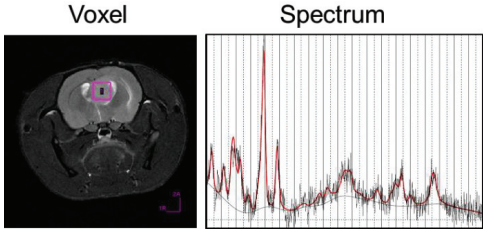

Fig 7 – Example of MRS spectrum of metabolites

Left panel: Reference T2 image of a rat implanted with a GBM, used to position the voxel in which metabolites concentrations are measured (purple square). Right panel: Spectrum acquired by SVS in the corresponding voxel. SVS: Single Voxel Spectroscopy.

Quantification was performed by comparing in vivo spectra with spectra obtained from solutions of individual metabolites, using the LCModel software [49].

Vessel architecture

Magnetic Resonance Angiography (MRA) was used to image healthy blood vessels in the brain and new forming angiogenic vessels in the tumor. The technique obtains images of flowing blood by saturating the MR signal in a slice to image prior to the acquisition, so that only unsaturated blood signal entering the imaged slice is seen during the acquisition, while the signal from all static tissue is not.

T2*-weighted, a variant of the T2-weighted protocol rendered sensitive to local field inhomogeneities, was used to image the presence of blood pools. The iron in blood creates distortion in the local magnetic field, so this kind of sequence can be used to image blood vessels as well. It can also be used to image the distribution of nanoparticles (small size particles with an iron oxide core and a biostable inert polymer coating) for angiography or molecular targets imaging applications.

Fig 8 illustrates the use of MRA and T2* after injection of nanoparticles to image vessels architecture and blood pools.

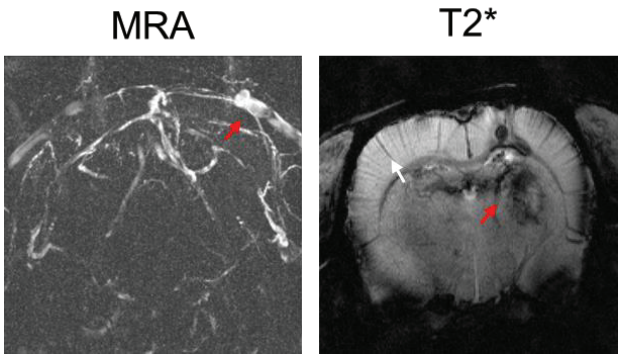

Fig 8 – Examples of MRI protocols used to image vessels architecture and blood pools

Left panel: Angiogram obtained by TOF-MRA of a rat with a GBM implanted in the right hemisphere, showing the presence of large angiogenic blood vessels at the periphery (red arrow). Right panel: T2* map obtained after the injection of nanoparticles (Ferumoxytol), highlighting the presence of blood vessels (white arrow) and the accumulation of the nanoparticles in tumor associated blood pools (red arrow). TOF-MRA: Time Of Flight – Magnetic Resonance Angiography.

Molecular imaging

PET protocols were used to assess glucose consumption and hypoxia. The protocols are detailed in the Materials and Methods sections of Paper III and summarized and illustrated below:

^{18}F-FDG PET was used to image the accumulation of glucose in the brain. The tracer accumulates in cells that avidly consume glucose such as glycolytic tumor cells but also highly replicative cells such as inflammatory cells.

^{18}F-FMISO PET was used to image hypoxic cells.

Fig 9 illustrates the use of ^{18}F-FDG PET and ^{18}F-FMISO PET to image glucose consumption and hypoxia respectively.

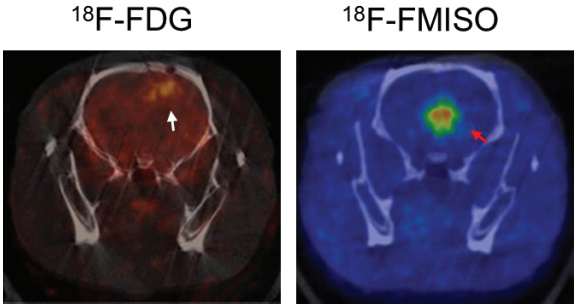

Fig 9 – Examples of PET protocols used to image glucose uptake and hypoxia

Left panel: SUV map obtained 30' after the injection of ^{18}F-FDG, used as a tracer of glucose uptake, showing tracer accumulation in the peripheral part of the tumor (white arrow). Right panel: SUV map obtained 120' after the injection of ^{18}F-FMISO, used as a tracer of hypoxia, showing important accumulation of the tracer in the central part of the tumor (red arrow). SUV: Standard Uptake Value, ^{18}F-FDG: ^{18}F-Fluorodeoxyglucose, ^{18}F-FMISO: ^{18}F-Fluoromisonidazole.

Table 3 here-after summarizes the imaging protocols used in the different studies

Study	Short description	T1c	T2	DCE	DWI	MRA	T2*	MRS	FDG	FMISO
1	Physiology	√	√	√	√			√		
2	Metabolomics	√	√					√		
3	Healthy animals		√					√		
4	Vascular normalization	√	√	√	√	√	√	√		√
5	Metabolic imaging	√	√						√	√

Table 3 – MRI and PET protocols used in the animal studies

3.1.3 Images quantification

Perfusion data analysis

The assessment of the physiological changes induced by bevacizumab was performed by DCE-MRI. This perfusion MRI technique relies on the intravenous injection of a bolus of contrast agent, followed by repeated acquisitions of fast T1-weighted sequences over time to establish the time course of contrast agent concentration. Unlike other perfusion techniques that limit acquisitions to the first pass of the contrast agent, we acquired data for an extended period of time to capture multiple passages of the contrast agent through the blood circulation.

We used an optimized version of a multi-compartmental pharmacokinetic model, known as the adiabatic tissue homogeneity model [62], to produce maps that represent the spatial distribution of four independent parameters: blood volume, blood flow, interstitial (extravascular extracellular) space fraction and blood-to-tissue transfer constant (Ktrans). In comparison to simpler models used in the clinic, such as the extended Tofts [63] model, this model provides access to blood vessel permeability parameters independently from blood flow and blood volume parameters. This choice of model was

important in order to distinguish the changes induced by bevacizumab on tumor perfusion itself from those related to the permeability of blood vessels.

The optimizations to the pharmacokinetic model are described in the Supplementary Materials and Methods of Paper II. Briefly, the model was optimized as follows:

- The Arterial Input Function (AIF) used to derive tissue impulse response function from contrast concentration curves, were extracted from contrast concentration curves using a single-channel blind estimation algorithm. This provides local AIF with reduced errors compared to AIF derived from nearby arteries or estimated by multichannel blind deconvolution [64].
- The convergence problem and incorrect parameters estimation induced by discontinuities in the adiabatic approximation to the tissue homogeneity model, caused by the discrete representation of the signal delay and mean capillary transit time, were addressed by using a distributed-capillary adiabatic tissue homogeneity model and continuous estimation of the delay in the Fourier domain [65].
- The pharmacokinetic modeling provides a set of interrelated values for the parameters of the response function and the AIF, but no scaling factor for the AIF. To obtain absolute values and allow inter-rats parameters comparison, we performed an additional scaling steps using reference values obtained from the literature for $v_p + v_e$ (plasma and interstitial space fractions) in the masseter muscles.

Fig 10 illustrates the perfusion and permeability parameters maps that can be obtained after pharmacokinetic modeling.

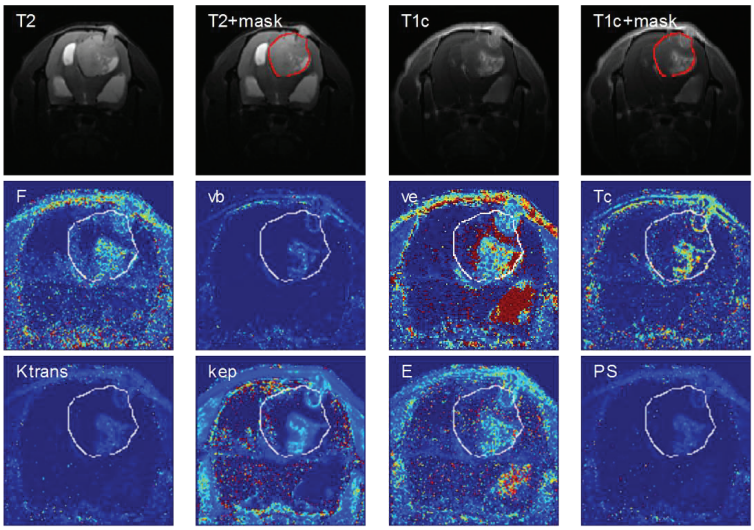

Fig 10 – Perfusion parameters maps obtained by DCE-MRI

T2 panel: Anatomical reference obtained by T2-weighted MRI, for a rat with a large GBM in the right hemisphere. T2+mask panel: Delineation of tumor ROI (red contour) overlaid to the T2-weighted sequence. T1c: T1-weighted sequence after injection of Gd-based contrast agent. T1c+mask panel: tumor

ROI (red contour) overlaid to T1-weighted sequence. Panels F to PS: Maps of perfusion parameters derived from DCE-MRI by pharmacokinetic analysis using the tissue homogeneity model [62]. The tumor ROI defined from the anatomical series (white contours) shows the heterogeneous values of the perfusion parameters in the tumor area. ROI: Region Of Interest, Gd: Gadolinium, DCE-MRI: Dynamic Contrast Enhanced – Magnetic Resonance Imaging, F: Blood flow, vb: Blood volume fraction, ve: Extravascular extracellular space volume fraction, Tc: Transit time constant, Ktrans: Vascular-to-interstitial space outflow constant, kep: Interstitial-to-vascular space backflow constant, E: Extraction fraction, PS: Permeability surface.

Diffusion data analysis

The Apparent Diffusion Coefficient (ADC) maps were calculated using the Image Sequence Analysis tool of Bruker's Paravision 5.0 software. Briefly, ADC is calculated from the equation

$$Y = A + I * \exp(-b * D)$$

where Y is the image intensity, A is an absolute bias parameter, I a multiplication constant, b is the diffusion b-value and D the diffusion constant. For different b-values (corresponding to different gradient strengths and delays), image intensity are recorded and a fit based on magnitude images of the reconstructed data is calculated. Because MRI is unable to differentiate diffusion-related motion from blood flow, perfusion, bulk tissue, or tissue pulsation-related motion, the diffusion value obtained is not an actual but an apparent diffusion coefficient or ADC.

PET data analysis

Mediso Nucline software was used for PET data reconstruction with correction for attenuation based on CT data. Mediso Inter View Fusion software was used for data visualization, co-registration of PET and CT data and quantification of standard uptake values as in [66].

Image processing

Perfusion, diffusion and metabolic PET imaging provided images that reflect the spatial distribution of directly quantifiable parameters. Anatomical MRI series (T1, T2, FLAIR) provided tissue contrast images reflecting proton density, weighted by relaxation parameters, for which direct interpretation and quantification is not straightforward. To quantify contrast enhancement, a differential image was used, obtained by subtracting T1 images obtained after and before injection of contrast agent with the exact same acquisition parameters.

The image processing and quantification typically included the following steps illustrated in Fig 11:

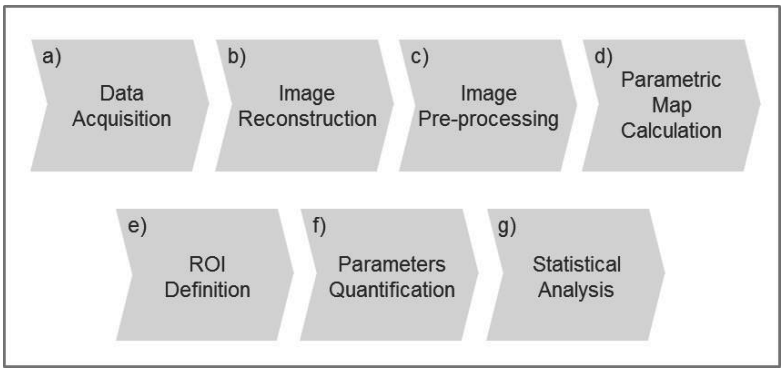

Fig 11 – Image processing and quantification steps (see text for description)

a) Data acquisition

Protocol setup and raw data acquisition were initiated from the operator's console attached to the imaging modality. For MRI, Paravison software from Bruker was used. For PET, Nanoscan from Mediso was used.

b) Image reconstruction

MR images are reconstructed automatically in Paravision by inverse Fast Fourier Transform of the data acquired in k-space, according to reconstruction parameters specified in the acquisition protocol. CT images acquired on the Nanoscan are reconstructed automatically as well. They were not used for quantification per se, but for attenuation correction when calculating PET Standard Uptake Values (SUV) images. Reconstruction of PET images leads to the creation of SUV maps, that represent the accumulation of the tracer in a given measurement period. Steps involved include the co-registration of PET and CT data, correction for attenuation of PET signal based on the x-ray attenuation provided by CT maps, and the specification of reconstruction parameters (field of view, binning, …)

c) Image pre-processing

When needed, the images were pre-processed using built-in functions from the Matlab image processing toolbox or features from Paravasion and Nanoscan. Possible pre-processing steps included:

- Denoising, using median filtering functions
- Resizing (or binning), to improve signal-to-noise ratio
- Affine transformation (translation, scaling, rotation)
- Registration
- Contrast optimization

d) Parametric map calculation

Perfusion raw data are T1-weighted images acquired over time. Maps of perfusion parameters (blood volume, blood flow, permeability parameters…) were calculated by first converting signal maps into contrast agent concentration maps, then by pharmacokinetic modeling as described in the 'perfusion data

analysis' section, using AIF extraction software and custom Matlab routines developed by collaborators of this project.

Apparent diffusion coefficient maps were calculated in Paravision from the diffusion images acquired at various b-values, reflecting gradients strength and duration.

No additional processing step was required for the PET SUV images.

e) ROI definition

The tumors used in this study have an angiogenic phenotype with limited infiltration and were therefore easily circumscribed on T2 and T1-weighted images after contrast injection. ROI's were defined for the tumor, contralateral hemisphere, muscle and whole brain. To facilitate the delineation of tumor in a given section, we used Matlab to display a montage of T1, T1c, T2 images for the given slice as well as previous and next slice, so that the tumor could be best visualized before delineation from the T2-weighted sequence.

Fig 12 illustrates the pre-processing and ROI definition steps performed in Matlab.

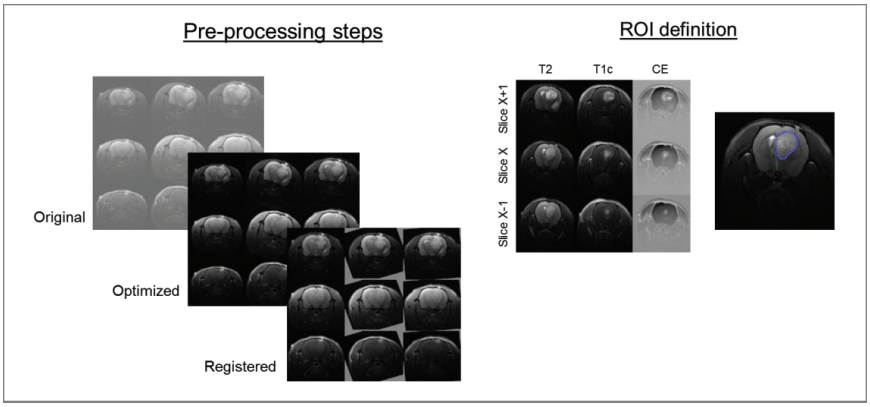

Fig 12 – Example of image pre-processing and ROI definition (see text for description)

f) Parameters quantification

Once all ROIs had been defined, parameters were quantified, including:

- Mean, standard deviation or other statistics for a given ROI
- Ratio of ROIs (f.i tumor vs. brain or tumor vs. muscle)
- Tumor pixels significantly changed (by selecting the intra-tumoral pixels whose values were statistically higher than values in the brain (i.e higher than mean + 3 * standard deviation)
- Histogram analysis

g) Statistical analysis

Statistical significance of change in the average value of parameters between the controls group and the treated group was typically evaluated by Wilcoxon rank-test or Analysis of variance accounting for factors such as tumor size or others, in addition to the treatment effect.

3.1.4 Biological assessment of tumor physiology

This thesis deals with the imaging of brain tumors and more specifically the use of imaging modalities to assess the physiology of brain tumors. A number of biological techniques were however also used by my collaborators in these projects to validate and further elucidate the imaging findings. The most important ones are briefly introduced in this section.

Histology and immunohistochemistry

Histology is a set of techniques used to evaluate healthy and pathological tissues and establish diagnosis in the clinic and in experimental settings. The most common approach is the staining of tissue sections (cryo-conserved or embedded in paraffin blocks) with hematoxylin and eosin (H&E). Hematoxylin colors the nuclei of cells (and few other objects) in blue, and eosin colors other cellular and extracellular proteins, highlighting the cytoplasm in pink and the blood cells in red.

More specific staining can be obtained with immunohistochemistry in which antibodies that bind specifically to proteins whose expression in tumoral tissue for example is of interest. The accumulation of the antibody in the tissue can then be visualized by tagging it to a fluorophore that will produce light detected by a fluorescence microscope when the fluorophore is excited with a laser beam operating at the proper frequency. Some of the antibodies used in these studies included:

- human-specific Nestin, a filament protein expressed by neural precursor cells, used to locate human tumor cells in rodent brain
- von Willebrand factor, a plasma protein expressed by endothelial cells and used to visualize the tumor vasculature
- Ki67, a nuclear protein found in proliferating cells
- Lactate dehydrogenase A (LDHA), an enzyme that catalyses the conversion of pyruvate to lactate, which we used to evaluate anaerobic glycolytic activity

Gene expression and copy number variation analysis

Altered gene expression is observed in many cancers and may influence treatment responses. The expression of targeted genes involved in angiogenesis and in cell proliferation pathways was assessed by Polymerase Chain Reaction (PCR), a molecular biology technique used to amplify copies of a piece of DNA, using primers (DNA fragments complementary to the target DNA) and a DNA polymerase enzyme to foster the DNA assembly from nucleotides.

We also used Array Comparative Genomic Hybridization (aCGH), a high-throughput technique used to compare a complete genome against a reference genome to identify normal and abnormal chromosomal copy number changes (deletion or duplications of certain regions of the genome). This was used to assess chromosomal aberrations in primary tumors (by comparison with healthy tissue) or in xenografts.

Protein analysis

Western blotting is a molecular biology method used to detect the presence of specific proteins in tissue extracts. By this technique, proteins of a tissue homogenate are separated by gel electrophoresis based on their size and electric charge, before they are transferred to a membrane where they are visualized and detected using antibodies specific to the target proteins. In our studies this was used to analyse the presence of Hypoxia Inducible Factor 1α (HIF1α), a protein which regulates the cellular response to hypoxia, or to assess the modulation of glycolytic enzymes as a response to anti-angiogenic therapy.

Metabolite analysis

To elucidate the metabolic changes induced by anti-angiogenic therapy, we used Liquid Chromatography Mass Spectrometry (LC-MS) of xenograft tumor and brain extracts, after the injection of glucose labeled with heavy isotopes of carbon (^{13}C). This analytical chemistry technique provides the possibility to detect and quantify the presence of chemicals with masses in a given range, for example metabolites, with high sensitivity and selectivity.

Metabolites are extracted from tissue homogenates and physically separated based on their traveling speed in a fluid that transport them through a column (liquid chromatography step). After separation, the chemical compounds are analysed and distinguished by their masses, providing spectra that show the distribution of chemical compounds in the sample (mass spectrometry step). Individual compounds can then be identified by comparing their position in the spectrum with the spectra from reference molecules acquired in the same conditions.

Molecules of interest labeled with heavy isotopes provide MS signals that can be distinguished from their unlabeled counterparts (because of slight differences in mass), making it possible to analyse the flux of the labeled molecules and their metabolic products, independently of the level of the unlabeled precursors and metabolites already present in the body.

Flow cytometric phenotyping

Flow cytometry is a cell assessment method, in which cells are suspended in a stream of fluid and analysed as they pass through laser beams. By labeling the cells with antibodies attached to fluorophores, it is possible to assess and quantify the subpopulations of cells in a sample that express cell surface proteins of interest. This was used to evaluate if the levels of cell membrane proteins or stem cell markers were modulated by anti-angiogenic therapy.

Cognitive function assessment

Long Term Potentiation (LTP) experiments were performed to assess changes in synaptic plasticity following anti-angiogenic therapy. This neuroscience technique measures the long lasting electrical response to stimuli using electrodes implanted in the hippocampus. The signal is associated with modifications of synaptic strength that underlie the mechanisms of learning and memory.

Histology, immunohistochemistry, gene expression analysis, protein analysis and flow cytometric phenotyping experiments were performed by colleagues at the Norlux laboratory of Neuro-Oncology, CRP Santé, Luxembourg, and at the Translation Cancer Research Laboratory at the Department of Biomedicine, University of Bergen, Norway. The metabolites analysis experiments were done in collaboration with the

Beatson Institute for Cancer Research, UK. The LTP experiments were done at the Neuroscience Research Group at the Department of Biomedicine, University of Bergen, Norway.

3.2 Experimental results

3.2.1 Paper I

Paper I is a review paper on the imaging of glioma in the context of molecular and cellular therapies, such as anti-angiogenic therapy that has been the focus of this thesis. The paper starts with an introduction on gliomas and the challenges associated with their treatment caused by their heterogeneity and the escape mechanisms that tumor cells are able to develop when challenged by conventional therapies. New treatment approaches are thus being investigated, including therapies with small molecules that interfere with the complex signaling associated with glioma development, inhibitors of angiogenesis and molecules that interfere with the impaired metabolism of tumors. Cellular therapies such as immunotherapies, gene and viral therapies, and strategies for the local delivery of therapeutic agents are presented as well.

The review discusses the imaging modalities and protocols that are used in the clinic today for the management of gliomas. MRI is presented as the modality of choice because of the wide range of soft tissue contrast mechanisms that it allows, which makes it possible to obtain anatomical, physiological and metabolic images all on the same modality. Nuclear imaging modalities such as PET or SPECT complements MRI by giving access to molecular processes associated with gliomas. Radiolabeled tracers that assess proliferation, metabolic activity and hypoxia are now commonly used in academic clinical settings.

Yet, no single modality is able to provide access to all the features relevant to glioma progression, and different challenges need to be addressed for the imaging of gliomas. One such challenge is pseudo-progression, an increase of MR signal caused by radiation-induced necrosis and inflammation that confound with tumor progression. Another challenge is pseudo-response, when contrast enhancement is strongly reduced following a therapy (such as a anti-angiogenic therapy) that modulate blood vessels permeability, despite the fact that the tumor keeps progressing in ways that may not have been captured by conventional imaging protocols. The invasive compartment of GBM is, in this respect, a challenge to image for the neuro-radiologist.

The paper then introduces pre-clinical imaging protocols currently under development, some of which being already used in clinical studies, and describe how these new protocols may be able to help addressing the challenges of glioma imaging in the future. The paper also addresses the technological advances that are likely to assist physicians dealing with gliomas in the context of the new therapies to come, by providing access to extended sets of disease relevant biomarkers.

New exogenous contrast agents, such as nanoparticles engineered for the imaging of receptors strongly expressed in GBM such as EGFR, VEGFR or integrin $\alpha_v\beta_3$ could have a role in the diagnostic and assessment of tumor progression. Endogenous contrast mechanisms such as the chemical exchange magnetization transfer of amide protons has shown promises for the detection of non-enhancing tumors and for the differentiation of tumor progression from radiation induced necrosis. Sequences that make use of blood-iron induced susceptibility changes such as Susceptibility Weighted Imaging have been proposed to assess microhemorrhages after radiotherapy, to grade intracranial tumors or assess responses to antiangiogenic therapy.

We also discussed how advances in perfusion imaging make it possible to assess blood volume, blood flow and vessel permeability simultaneously, some of these markers being used to grade tumors and assess the early response to therapy. Water molecule diffusion techniques that are able to distinguish the contributions from hindered and less restricted water molecules can help separate regions of infiltrating tumors from peritumoral edema. Diffusion techniques with oscillating gradients promise to assess changes in microstructures that would indicate response to treatment much earlier than changes in cell density.

Advances in magnetic resonance spectroscopy and chemical shift imaging, using multinuclear spectroscopy and spectral editing techniques will facilitate the use of metabolites levels and ratios to characterize tumors and assess response to therapy. Hyperpolarization of exogenous compounds followed by the tracking of these compounds and their metabolites is a very promising technique. Pre-clinical proof-of-concept studies have started to show its utility to assess a diverse range of tumor features such as glucose metabolism, cell death, redox state or IDH mutation status.

PET and SPECT tracers are used to image cellular death, tumor vasculature, immune response, molecular targets and pathways and drug delivery.

Paper I also addresses how technological advances in high field magnets, parallel imaging and fast imaging techniques as well as hybrid modalities systems will advance the field of brain tumors imaging. The combination of the information coming from different modalities and protocols will require processing by advanced data analysis techniques, such as pharmacokinetic modeling, advanced image processing, tumor growth modeling, visualization techniques, virtual and augmented reality, omics data integration and computer-assisted decision making. This is summarized in the conceptual framework for brain tumor data management presented in Fig 13, reproduced from Paper I.

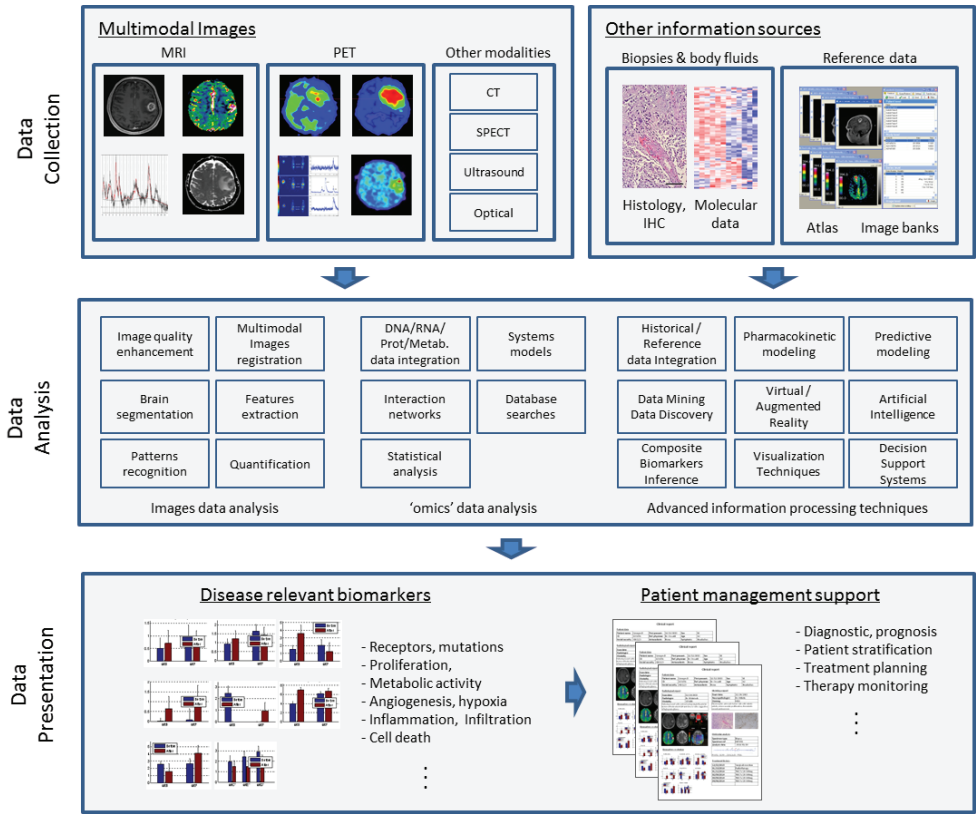

Fig 13 – Conceptual framework for brain tumor data management

The use of imaging and non-imaging data to support the management of brain tumors can be envisaged as a multi-step process. First, anatomical images of the brain obtained by MRI are completed by images that represent the spatial distribution of physiological parameters related to perfusion, metabolic activity or the level of molecular targets, assessed by MRI, PET and possibly other imaging modalities. The second step is the combination of this multi-parametric data with non-imaging data coming from the histological and molecular analysis of biopsies and body fluids, possibly compared to historical and external reference data when available. Advanced information processing techniques used at this stage may include images features extraction, biological networks analysis, pharmacokinetic and tumor growth modeling, advanced data discovery and presentation techniques. The ultimate goal of the analysis is to provide the physician dealing with the patient a set of validated disease relevant biomarkers, that will be used when key decisions are to be taken, such as to establish diagnosis and prognosis, to stratify patients to therapy, to plan treatment and monitor its efficacy.

3.2.2 Paper II

Paper II reports on the biological, physiological and metabolic changes induced by treating a patient-derived xenograft model of GBM (P3) with the anti-VEGF agent bevacizumab. The key findings in this study were that:

1. The strong contrast reduction observed in our glioma model (similar to what is observed in clinical settings) is associated with a strong decrease in the permeability of the blood vessels as determined by perfusion MRI.
2. In addition to the reduction of blood vessels permeability, we also found a significant reduction in the blood supply to the tumor, an observation of clinical relevance, notably for the delivery of chemotherapeutic agents.
3. An increase in tumor hypoxia is also observed as well as the activation of pro-angiogenic pathways.
4. Another consequence of the reduced blood supply to the tumor appears to be an increase of the glycolytic metabolism of tumor cells after the treatment with bevacizumab. This metabolic adaptation may result in increased acidification of the microenvironment, facilitating the infiltration of tumor cells in the parenchyma.

Those findings are further developed in the following paragraphs.

Contrast enhancement, permeability of blood vessels, and tumor perfusion

The impact of anti-VEGF treatment on contrast enhancement was assessed using P3, a GBM model that had previously been shown to display an angiogenic phenotype with endothelial cells proliferation confirmed by histology [60, 61]. As expected, and similar to the general findings in the clinic, bevacizumab induced a strong reduction in contrast enhancement (Fig 14).

Maps of perfusion and blood vessel permeability parameters were produced by pharmacokinetic modeling of DCE-MRI data, and statistical analysis was performed in regions of interest drawn on the tumor using T2-weighted and T1-weighted after Gadolinium contrast agent injections sequences. Statistical tests used included Wilcoxon rank-sum tests and ANOVA (analysis of variance) using the treatment, tumor volume and animal weight as factors. As expected, we found that permeability parameters and blood volume were strongly reduced in bevacizumab treated animals, explaining the strong reduction of contrast enhancement observed in T1-weighted MRI series. These experimental results correlate well with clinical findings reported in the literature [17, 18]. Radiological response is instrumental to the assessment of response to therapy in clinical studies on brain tumors, and end points based on changes in contrast enhancement are used in the clinic, including in the clinical studies on the basis of which the FDA granted accelerated approval for the use of bevacizumab for the second line treatment of GBMs [67].

Interestingly, we also found that blood flow was significantly reduced in the treated animals. Blood flow parameters are more seldom reported in the literature than blood volume parameters, in part due to the fact that models used in the clinic are often based on DSC-MRI and the first pass of the bolus of contrast agent, which do not properly account for the leakiness of tumor blood vessels. Our results thus appear to contradict the hypothesis of 'vascular normalization' induced by anti-angiogenic therapies, which suggests that blood flow could be improved as a result of the vascular normalization [13]. We instead proposed the

normalization to be 'morphological' (reduction of the number of large aberrant blood vessels in the tumor), rather than 'functional' (which would have resulted in improved blood supply to the tumor).

Fig 14, adapted from Paper II, illustrates the reduction in parameters related to tumor perfusion and permeability of blood vessels induced by the anti-angiogenic therapy with bevacizumab

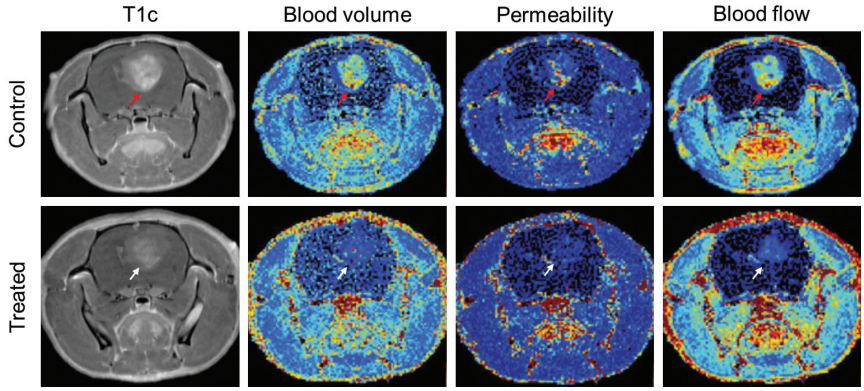

Fig 14 – Bevacizumab decreases contrast enhancement, perfusion and permeability parameters

Maps representing contrast enhancement, blood volume, permeability and blood flow for the P3 patient-derived xenograft model. For the control animals (top row), high contrast enhancement, blood volume, vessel permeability and blood flow values are observed in the tumor (red arrows). In contrast, animals treated with bevacizumab (bottom row) show more homogeneous and lower values for contrast enhancement, perfusion and vessel permeability parameters (white arrows).

Tumor hypoxia and activation of angiogenic pathways

Several findings in the studies we performed suggest that hypoxia might be increased when treating the animals with bevacizumab. We showed that the level of HIF1α, a protein that regulates response to hypoxia in normal and pathological cellular processes [68], is increased in bevacizumab treated animals compared to controls, as assessed by Western Blots. The gene coding for this protein was also upregulated as determined by real-time PCR.

Another indirect evidence came from the analysis of metabolites in vivo by Magnetic Resonance Spectroscopy. We found an accumulation of lactate, alanine, choline, myo-inositol, creatine, taurine and mobile lipids in the treated animal, a combination that has previously been associated with increased hypoxia in human brain tumor spectra [69].

Gene expression analysis of the xenografts also revealed an activation of angiogenic pathways as a result of bevacizumab treatment. Transcripts such as angiopoietin 2, endothelial tyrosine kinase and VEGF-A were strongly upregulated in the treatment group. Although genes related to other survival mechanisms were not specifically assessed, the real-time PCR analysis also suggested that genes associated with autophagy were also over-expressed as a result of the bevacizumab treatment (Abdulrahim et al, manuscript in preparation).

Glycolytic metabolism

Several results in the study indicate that anti-VEGF treatment might increase the glycolytic metabolism of the tumor cells. The first evidence came from the *in vivo* assessment of metabolites in the tumors by MRS. We found lactate, the end product of anaerobic respiration, to be significantly increased in the treated tumors. This increase in lactate and the changes in other abundant metabolites were also confirmed by NMR and GC-MS of tumor samples extracted at the end of the study (Data not published, courtesy of Mattias Hedenström and Henrik Antti, University of Umeå).

Invasion of tumor cells

Increased acidity in the brain parenchyma, as a result of abundant lactate production, may favor tumor cell invasion [70]. We thus assessed the infiltration of tumor cells by histology, after staining sections with an antibody against human-specific Nestin, a protein expressed in the vast majority of GBMs cells. Images were randomly taken with a microscope at different locations at the periphery of the tumors. A small script written in ImageJ was then used to count the number of Nestin positive pixels distant from the tumor core. We found a strong increase in the number of infiltrating cells (68%, $p<0.001$) in the bevacizumab treated animals, compared to the controls. The distance of infiltrating cells from the tumor core was also strikingly higher.

Infiltrating tumor cells are difficult to assess with MRI which lacks the sensitivity of PET in this respect. Since we didn't have access to a PET modality at the time of this study, we evaluated whether Diffusion Weighted Imaging (DWI) could give us indications about the infiltrative nature of the tumors. It had previously been proposed that the Apparent Diffusion Coefficient calculated from DWI correlates with cellularity [71, 72], and that non enhancing tumor progression could be detected using ADC histograms [73]. Using ROIs drawn from the contrast enhancing region of the tumors, as determined from T1-weighted sequences after injection of contrast agent, to which we added a small margin, we calculated the number of pixels in the margin area that displayed low ADC values. We found this number to be more elevated in the bevacizumab treated animals, thus correlating with the results provided by the Nestin staining.

Fig 15 illustrates the approaches used to quantify tumor cell infiltration by histology and DWI.

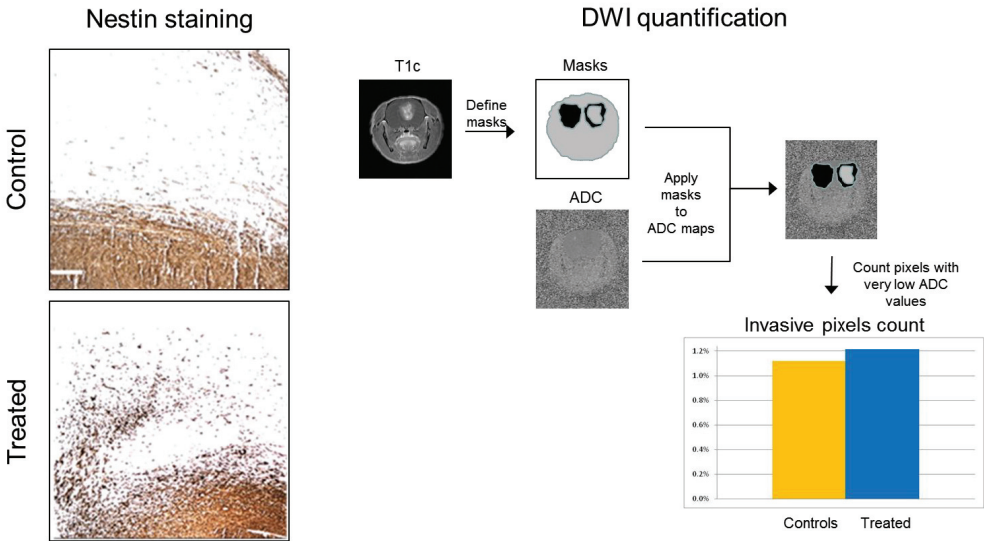

Fig 15 – Approaches used to assess tumor cell infiltration

Left column: Immunostaining of paraffin sections with Nestin, a human-specific protein expressed in nerve cells, that we used to locate tumor cells originating from the patient in host stromal tissue. Image from a representative animal treated with bevacizumab (bottom panel) shows increased invasion of tumor cells in the parenchyma in comparison to control animals (top panel). Right column: Quantification approach of invasion based on DWI MRI. T1c sequences, acquired after the injection of Gd-based contrast material were used to define masks of tumor and normal brain. Masks were then applied to ADC maps and pixels with very low ADC values in the tumor periphery (in comparison to normal brain), were counted and served as a basis to quantify tumor cell infiltration

3.2.3 Paper III

In this paper, we report the results of experiments that were performed to validate the findings described in Paper II and further elucidate the mechanisms of metabolic adaptation. To this end, we:

1. Reproduced the histological and radiological studies using a second patient-derived GBM xenograft model (P13) with established angiogenic features
2. Performed a metabolomic study of the tumor and brain extracts from animals treated with bevacizumab, using labeled ^{13}C glucose and LC-MS
3. Assessed glucose uptake and hypoxia in vivo using PET imaging

The results of these experiments are summarized in the following paragraphs.

<u>More evidences of increased hypoxia in the tumor</u>

The longitudinal changes in hypoxia induced by bevacizumab were assessed in vivo using ^{18}F-FMISO PET imaging. We found FMISO uptake in the tumor to increase steadily in both the P3 and the P13 tumor models, as early as 1 week after the start of treatment. Hypoxia kept increasing over time.

Fig 16 illustrates the sharp increase in hypoxia in bevacizumab treated animals.

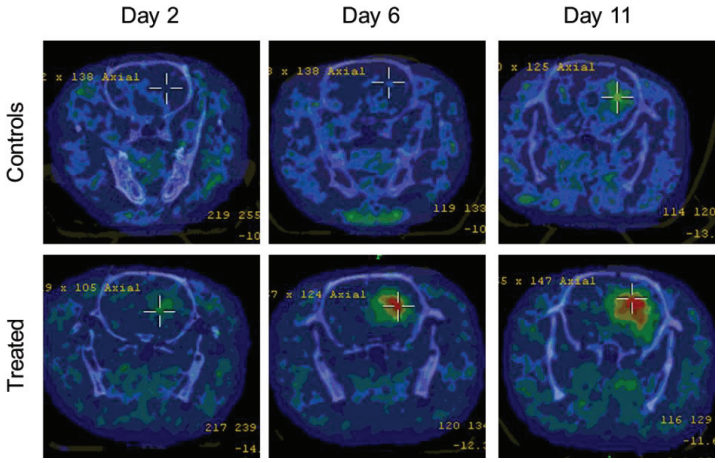

Fig 16 – Increase in hypoxia after anti-angiogenic therapy

SUV of ^{18}F-FMISO, used as a PET tracer for hypoxia, 120' after the intravenous injection of the tracer, for a representative P13 patient-derived xenograft from the control group (top row) and the bevacizumab treated group (bottom row) at day 2, 6 and 11 after the start of the treatment which consisted of saline injections for the controls and bevacizumab for the treatment group. The control animals show a limited increase in hypoxia over time, while the treated animals showed elevated hypoxia (red areas), starting early after the beginning of the treatment. SUV: Standard Uptake Value, ^{18}F-FMISO: ^{18}F-Fluoromisonidazole, PET: Positron Emission Tomography.

Although the small number of animals in the study was not sufficient to allow proper statistical testing, the same pattern was consistently seen in all treated animals, while controls demonstrated a more irregular and less pronounced progression.

Confirmation and elucidation of the metabolic adaptation

To confirm the increased production of lactate following anti-VEGF treatment, we first assessed the expression of the enzyme lactate dehydrogenase (LDHA) in the treated animals by immunohistochemistry and by western blots. In a series of biopsy specimens from GBM patients, collected before and after bevacizumab treatment, we also found the number of LDHA positive cells to be significantly increased after treatment both in the center of the tumors as well as in diffusely infiltrative regions.

Yet, the most striking evidence of increased glycolytic metabolism in the bevacizumab treated animals came from the metabolomics study. Animals implanted with the P3 tumor model, were treated with bevacizumab for 3 weeks. They then received an injection $^{13}C_6$-labeled glucose, 15' prior to sacrifice, and the tumor samples were extracted and analysed by LC-MS. We found the pool of unlabeled glucose and pyruvate to be reduced after treatment, suggesting an increased glycolytic metabolism in the tumor of animals treated with bevacizumab. We also found an increased influx of labeled glucose in the treated animals resulting in an increased production of labeled pyruvate and lactate. The increase in glucose uptake after treatment was also observed *in vivo*, using ^{18}F-FDG PET, and we observed an up-regulation of key enzymes associated with glycolysis using qPCR analysis.

In contrast, metabolites associated with the TCA cycle, such as cis-asconitate, α-ketoglutarate, succinate, fumarate and malate were significantly down-regulated in the bevacizumab treated animals compared to controls. PDK1, an inhibitor of PDH and regulator of the flux to the TCA cycle, was increased suggesting a partial shutdown of the TCA cycle in favor of lactate dehydrogenase activity, resulting in increased lactate production and depletion of the glucose and pyruvate pools.

These findings, summarized in Fig 17, adapted from Paper III, suggest that bevacizumab treatment causes an increased use of glycolytic metabolism.

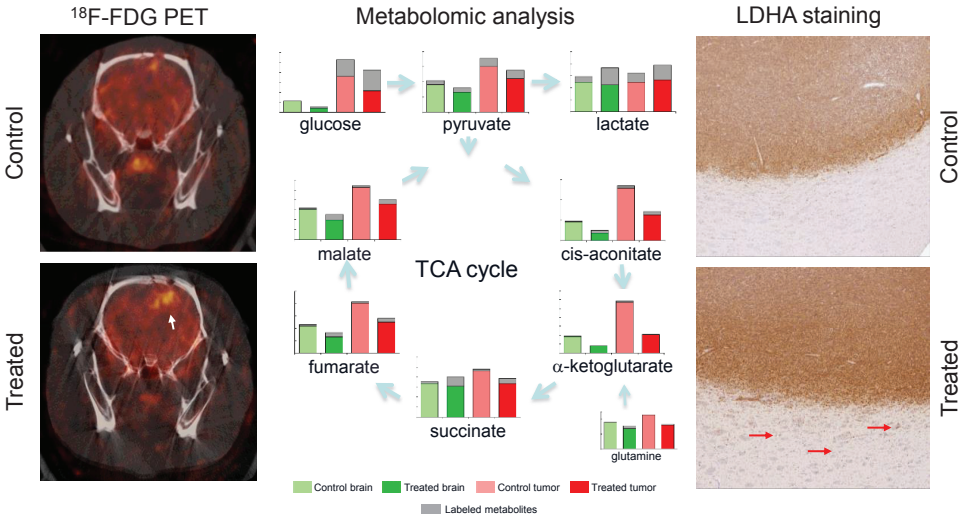

Fig 17 – Evidences of increased glycolytic metabolism in bevacizumab treated animals

Left panels: SUV of ^{18}F-FDG, used as a PET tracer for glucose uptake, 30' after the intravenous injection of the tracer, for a representative patient-derived xenograft from the control group (top row) and the bevacizumab treated group (bottom row). Maps show areas of more pronounced glucose uptake (white arrow) in the animals treated with bevacizumab. Middle panels: Metabolomic analysis of TCA cycle metabolites quantities, 15' after injection of ^{13}C-labeled glucose. Glucose and pyruvate pools are depleted as a result of increased glycolysis in bevacizumab treated animals. In contrast, the concentration of metabolites of the TCA cycle is reduced, suggesting an increased use of anaerobic respiration for energy production. Light green bar: Untreated normal brain, Dark green bar: Normal brain treated with bevacizumab, Light red bar: Untreated tumor, Dark red bar: Treated tumor. Grey bar: Labelled metabolite. Right panels: Immunostaining of paraffin sections with LDHA, the enzyme involved in pyruvate to lactate conversion, showing high expression in the tumor region in both control and bevacizumab treated animals. The staining also appears more pronounced at the periphery of the tumor for treated animals as well as in infiltrating cells (red arrows). SUV: Standard Uptake Value, ^{18}F-FDG: ^{18}F-Fluorodeoxyglucose, PET: Positron Emission Tomography, TCA: Tricarboxylic Acid, LC-MS: Liquid Chromatography-Mass Spectrometry, LDHA: Lactate Dehydrogenase A.

3.2.4 Paper IV

This paper presents preliminary results of experiments performed on healthy animals to determine whether treatment with anti-VEGF could induce a decline in neurocognitive function.

Decline in neurocognitive function

Results from a recent large scale clinical study evaluating bevacizumab in patients with newly diagnosed GBM indicated that patients treated with bevacizumab showed a decline in global neurocognitive function

compared to untreated patients [74]. Since, in addition to its role in vascular development, VEGF is also known to be important for neuronal activity [75], providing neuroprotection from hypoxia and trauma [76-78], we performed studies to examine whether this decline in neurocognitive function could be corroborated in our animal models.

We show that, after treating healthy rats with bevacizumab for a 3 weeks period, in addition to the genes important for endothelial function and development, genes involved in CNS function and development were significantly deregulated in the bevacizumab treated animals compared to controls. We also performed a long-term potentiation experiment (LTP), to determine dynamic neuronal plasticity changes in the hippocampus. It had previously been reported that VEGF increases LTP in the CA1, a region that plays an important role in spatial learning and short term memory function, and that the absence of VEGF abrogates this effect [79]. In our study with healthy rats, we found that treatment with bevacizumab caused a strong reduction in LTP compared to the controls animals, supporting the hypothesis of a possible reduced neurocognitive function after bevacizumab treatment.

3.2.5 Unpublished results

Finally, during the course of our experiments we investigated additional aspects related to the response of GBM to anti-VEGF therapy, notably we started to address the following questions:

1. Does treatment with anti-VEGF therapy provide benefits at all in terms of overall survival
2. Is there a 'window of normalization' of the tumor vasculature shortly after the start of the treatment, as suggested by other research groups, that could be exploited to improve the efficiency of radio and/or chemotherapy?

Preliminary results suggest that, similarly to the clinic, a small benefit in overall survival can be observed in some GBM models. The vascular normalization window was however not found in our P3 and P13 models up to now. The preliminary results are presented here-after, but will need confirmation before they can be proposed for publication.

Tumor growth and survival

In the study described in Paper I, on the physiological changes induced by anti-angiogenic therapy, animals were implanted with the P3 model, and sacrificed at the end of the 3 weeks treatment period. The tumor doubling time measured from the treatment start point to the sacrifice time point was 16% longer in the animals treated with bevacizumab ($p<0.05$) than in the controls, indicating a slow down of tumor progression, as measured by the visible part of the tumor on T1-weighted after contrast and T2-weighted images.

In an ongoing study on vascular normalization, we continued the treatment of the animals that were still alive at the end of the initial 3 weeks treatment period, until neurological symptoms appeared. This study was performed with both the P3 and the P13 models. The animals in the treatment group survived 24% and 20% longer than those in the control groups, for the P3 and P13 models respectively. The difference in survival duration was statistically significant for P3 animals ($p<0.05$) but not for P13 animals. Thus, in our animal models, bevacizumab may provide a small survival benefit, at least in some of the animals.

Fig 18 shows the Kaplan-Meier survival plots for the P3 and P13 animals of the vascular normalization study.

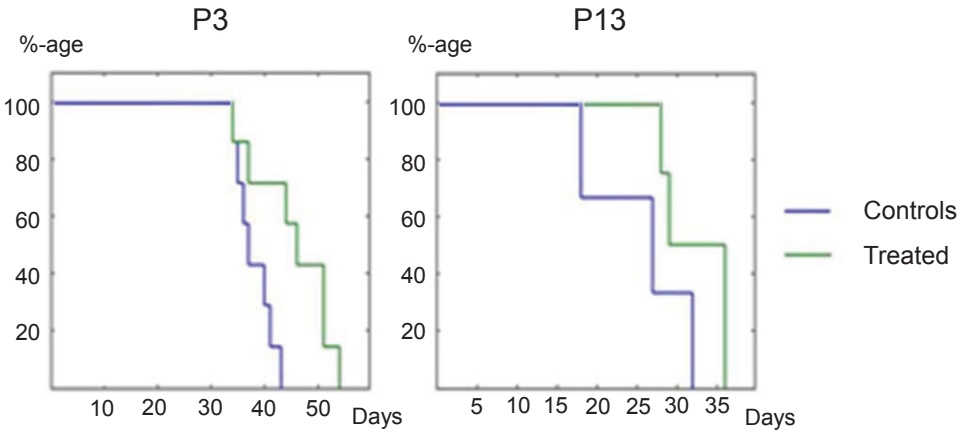

Fig 18 – Bevacizumab treatment may provide survival benefit

Kaplan-Meier survival curves comparing survival in our patient-derived xenograft models (P3-left panel, P13-right panel) for control animals (blue line) and animals treated with bevacizumab (green light), showing a tendancy toward increased survival for the treated animals. The difference was statistically significant for the P3 model but not for the P13 model which was performed with a smaller set of animals (<10).

Vascular normalization

The results on perfusion changes induced by Anti-VEGF treatment we reported in Paper II were acquired after 3 weeks of treatment. At this advanced stage of tumor development, vessel pruning had happened, as evidenced by the immunohistological analysis of blood vessels using von Willebrand Factor staining. To examine whether a 'window of vascular normalization' possibly exists at some stage during the treatment, we have initiated a study to assess perfusion parameters changes during anti-angiogenic therapy longitudinally, using the P3 and P13 models. Preliminary results suggest that blood flow fluctuates over time, with a tendency to increase in the control animals and a tendency to stabilize or decrease for bevacizumab treated animals. No window of vascular normalization associated with improved blood flow has been observed after bevacizumab treatment so far in our models.

Fig 19 illustrates the longitudinal changes induced by anti-angiogenic therapy for representative animals from the control and bevacizumab treated groups in the vascular normalization study (data not published).

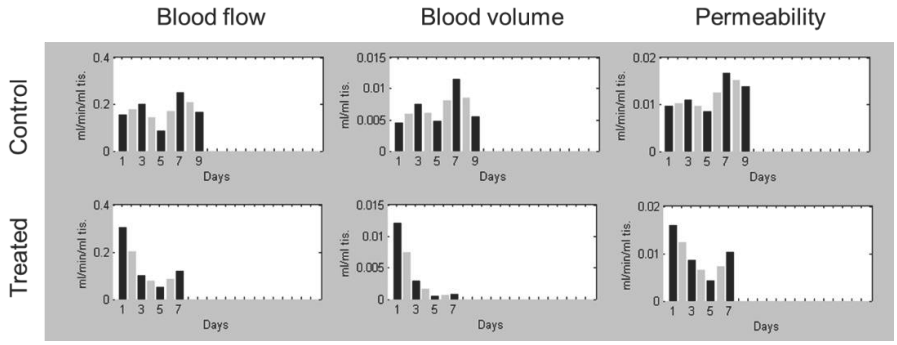

Fig 19 – Longitudinal changes in perfusion and permeability parameters induced by anti-angiogenic therapy

Blood flow, blood volume and permeability parameters were measured every other day (black bars) for P3 patient-derived xenografts. Grey bars represent calculated intermediary values of the parameters and are used to illustrate daily changes, in one representative animal of the controls group (top row) and one of the bevacizumab treated group (bottom row). Control animals show fluctuating values over time for perfusion and permeability parameters with a tendency to increase over time. Bevacizumab treated animals in contrast show less fluctuations and a tendency to decrease over time. X-axis represent days from treatment start, Y-axis represent absolute values in blood flow, blood volume and permeability (Ktrans) parameters.

4 DISCUSSION

In May 2009, the FDA granted accelerated approval for bevacizumab (Avastin®, made by Genentech, Inc), a monoclonal antibody against VEGF-A, to be given as a single agent to GBM patients that have progressive disease following prior therapy. The approval was based on the results of two small phase II clinical trials, AVF3708g and NCI06-C-0064E, which demonstrated improved progression free survival in comparison with historical data, when the treatment was given as monotherapy [17, 18]. The efficacy of bevacizumab was assessed using the WHO radiographic criteria [80], whereby increase in contrast enhancement was measured on MRI every 4 to 6 weeks after the start of the treatment. A new area of nonenhancing T2 or FLAIR signal consistent with tumor presence was also considered as progressive disease.

Since the approval of bevacizumab by the FDA, concerns have been expressed about the real anti-tumor efficacy of the drug. Despite an initial improvement in patient conditions [81], most likely consecutive to reduced cerebral edema, intracranial pressure, and reduced use of corticosteroids, the tumor apparently continues to progress and the benefit related to overall survival is generally marginal. Based on prior knowledge, it is highly likely that adaptation mechanisms take place that might involve activation of other pro-angiogenic factors [82] and/or infiltrative progression [83, 84], limiting therapeutic efficacy [85-88].

In Europe, the EMEA did not grant approval for bevacizumab treatment based on lack of clear evidence of clinical benefits [89]. Recently, results from two major phase III clinical trials, the RTOG 0825 and AVAglio, in which bevacizumab was used as first line treatment of GBM, did not report any significant benefit in overall survival either [23, 24]. These trials showed that the toxicity of bevacizumab is relatively low. Still, in a meta-analysis of cancer patients treated with bevacizumab, an increased risk of fatal adverse events were reported compared to patients treated with chemotherapy alone [90], with bevacizumab increasing the risk of ischemia [91, 92] and serious hemorrhage [93]. The RTOG 0825 also reported a decline in neurocognitive function and quality of life in patients treated with bevacizumab for long periods, in comparison to controls.

Globally, these findings question the exact role of bevacizumab in the treatment of glioblastoma [94, 95] and the need of the current imaging protocols to evolve to better assess response to treatment in the context of anti-angiogenic therapies [96]. The present thesis was initiated to try and address some of these questions.

4.1 Investigating physiological changes induced by anti-angiogenic therapy

First of all, the frequent failures of drugs that perform well in vitro and in pre-clinical settings, once they are transferred to the clinic, raise the question of the adequacy of the animal models used to predict a potential therapeutic response in humans.

Using the GBM patient-derived xenograft model introduced in paragraph 1.4, we have found that overall survival was only marginally improved in tumor bearing animals treated with bevacizumab, despite a strong reduction of contrast enhancement observed by MRI. Evidences from gene expression and molecular analyses support the hypothesis that adaptation mechanisms indeed take place, resulting in the activation of pro-angiogenic pathways and increased invasion of tumor cells into the brain parenchyma. In a study on neuronal plasticity in the hippocampus of healthy rats treated with bevacizumab, we also found a reduction of long term potentiation in neurons which could be associated with the cognitive impairment observed in the RTOG 0825 study.

Altogether, these findings suggest that the animal model used in our studies is able to reproduce the observations seen in the clinic, thus providing a solid basis to study the effects of anti-angiogenic therapy.

In addition to our findings, confirming the similarity of features in the animal xenograft model and in GBM patients, our results also show an increased use of the glycolytic metabolism caused by bevacizumab therapy. This observation is new. We show that the increased glycolytic activity is related to a reduction of blood supply to the tumor leading to an increase in intratumoral hypoxia, which we demonstrated by MR spectroscopy, perfusion MRI and PET imaging with ^{18}F-FDG and ^{18}F-FMISO. The increased acidification of the microenvironment resulting from the accentuated glycolytic metabolism may provide the ground for an increased infiltration of tumor cells in the brain parenchyma observed in the clinic [97-99] and which we reported in Paper II and Paper III.

4.2 Radiological assessment of response to anti-angiogenic therapy

Given the discrepancy between the strong radiological changes observed after anti-angiogenic therapy and the lack of benefit in patients overall survival, the medical and scientific community is questioning the adequacy of the protocols currently used in the clinic to properly assess the efficacy of this type of therapy.

Recently, an international panel of experts, the RANO group, has reviewed the response criteria for brain tumors, and judged the response rate and progression-free survival as inappropriate end points for anti-VEGF treatments [100]. Updated response assessment criteria for high-grade gliomas were proposed [101], in which T2/FLAIR sequences complement the information provided by the unspecific contrast detected in T1-weighted sequences after injection of Gadolinium-based contrast agents. This addition was proposed to help addressing the problems of pseudo-progression (when radiation induced necrosis is confounded with tumor recurrence) and pseudo-response (when anti-angiogenic agents reduce contrast enhancement despite continued tumor progression). Several authors have also proposed that perfusion and diffusion sequences could be used to assess the changes induced by conventional and anti-angiogenic therapies in a more quantifiable manner [102-107].

Our studies reported reduction in contrast enhancement following bevacizumab therapy as well, and similarly to clinical findings, this lead to only marginal improvement in overall survival. We additionally showed that the reduction of contrast is associated with a strong reduction of the permeability of blood vessels determined by DCE-MRI. Most clinical studies that study perfusion in the brain use DSC-MRI of the first pass of a bolus of contrast agent injected intravenously. The alternative method used in our studies, DCE-MRI of the multi pass of the contrast agent, may have advantages over DSC-MRI in this context. The key benefit being the ability of DCE-MRI and multi-pass bolus approaches to provide access to perfusion and blood vessel permeability parameters separately.

Blood volume parameters can be evaluated reliably by both methods and the value of this parameter in predicting tumor grade, evaluating treatment efficacy and differentiating recurrence from radiation necrosis is gaining acceptance [38, 39, 103, 108]. Yet, other parameters such as blood flow and permeability of blood vessels, that are best evaluated by DCE-MRI [109-112], also bear clinical importance as they relate to the delivery of chemotherapeutic agents and contrast agents to the tumor. This additional information is especially important in the context of anti-angiogenic therapies which are known to modify the permeability of blood vessels [109, 113]. DCE-MRI however comes at the expense of longer acquisition times and more complex pharmacokinetic modeling. Therefore, careful planning may be required if such sequences are to be added into an already busy schedule, to avoid increasing the scan

time over what is acceptable for patients that are already in poor clinical condition. Dual echo perfusion MRI techniques, assessing the T1 and T2 effects simultaneously may provide improved separation of perfusion and leakage parameters [114, 115].

As discussed in Paper I, several techniques, currently used in experimental settings and in clinical trials, may also enhance our ability to assess responses to molecular and cellular therapies in the future. Among these, Diffusion Weighted Imaging has started to show value in assessing responses to anti-angiogenic therapies: Histogram analysis of ADC data can assist in predicting survival [116], and Restriction Spectrum Imaging, a technique that distinguishes slow from fast diffusion components such as, respectively, infiltrating tumor cells and edema, was shown to be resistant to pseudoresponse in patients with high grade gliomas treated with bevacizumab [117]. Susceptibility Weighted Imaging has also been proposed to study the microvasculature of tumors in anti-angiogenic or combined therapies [118-120]. BOLD fMRI can be considered to analyse tumor hypoxia [121, 122] or vessel maturity [123], and spectroscopy techniques are investigated for their ability to detect glycolytic activity [124], IDH mutation [125] or to provide early markers of responses to anti-angiogenic therapy [126, 127], with preclinical protocols using hyperpolarized compounds showing promises as well [128]. PET tracers of proliferation can also prove useful in the context of anti-angiogenic therapies [129, 130]. In Paper I, we reviewed these techniques and discussed their use at various stages of glioma management. Which of these techniques will be used in the clinic in the future is not clear. MRI-based techniques can be easily deployed once they are validated. PET tracers come with more logistical constraints but retain the advantage of their very high sensitivity.

4.3 Infiltrative progression pattern

There is a controversy about the fact that treating GBM with anti-angiogenic therapies may increase the infiltration of tumor cells into the brain parenchyma [98, 99, 131, 132]. Our studies in preclinical GBM models provide new insight into the mechanisms of adaptation to anti-angiogenic therapy that can favor this infiltrative progression. In this respect the observations made in GBMs may not really be different from what has been reported for non cranial tumors, such as colorectal cancer, metastatic breast cancer, non-small-cell lung cancer or renal cell carcinoma, treated with anti-VEGF agents. In a recent review, a meta-analysis of clinical trials reported that benefits in progression-free survival for patients treated with anti-VEGF compounds were not accompanied with increased overall survival. For these tumors as well, anti-angiogenic therapy may lead to a more invasive or metastatic behavior [133].

The MRI protocols in use in the clinic today lack the sensitivity required to detect these infiltrative patterns. FLAIR has been proposed to assess tumor progression beyond contrast enhancement, but the signal abnormalities that can be observed in the tumor region and in its surroundings, using these protocols, are unspecific. Diffusion sequences can be considered to assess the response to angiogenic therapies [134, 135]. The interpretation of diffusion weighted images in the context of anti-angiogenic therapies is however challenging because hypercellularity on one hand, edema and necrosis on the other hand, can all affect the diffusion of water molecules in different ways. Experimental techniques, such as the previously mentioned Restricted Spectrum Imaging [117] may help resolve this issue in the future. Magnetic resonance diffusion imaging with oscillating gradients could also be considered, since this technique may be able to detect changes in intracellular structures that may precede changes in cellularity [136].

In Paper I, we have discussed other techniques that could help addressing the imaging of the infiltrative component. Amide proton transfer, a CEST MRI technique, could be considered for this purpose and has shown promises in preclinical and clinical studies for the detection of tumors and the differentiation of tumor recurrence from radiation necrosis [137-140]. By producing contrast from endogenous molecules rather than from exogenous contrast agents injected intravenously, this technique is independent of the delivery of a tracer and the possible changes in the permeability of blood vessels. Nanoparticles directly targeting infiltrating cells or indirectly detecting their presence by probing angiogenic endothelial cells, matrix remodeling or immune response activity, could also play a role if they can be engineered to efficiently home to specific targets, behind an intact blood-brain-barrier. But because some of these targets may be present at very low concentrations, imaging techniques with exquisite detection sensitivity, such as PET or SPECT, may retain a certain advantage in these scenarios [141, 142].

4.4 Combination therapies

Can the efficacy of anti-angiogenic therapy be improved by its combination with drugs that target the mechanisms of adaptation that the tumor develops?

There are no reports on GBM patients who have been cured by anti-angiogenic therapy. All patients develop some form of resistance to the treatment. The mechanisms of resistance may include the activation of alternative pro-angiogenic pathways, the recruitment of circulating endothelial cells towards the tumor [97] or, as proposed in Paper III, the up-regulation of molecules leading to increased glycolytic activity and infiltrative tumor growth. Similar results were observed in clinical trials with anti-angiogenic therapies using other vascular targets, in which resistance to therapy was reported as well [143, 144]. Since only a subset of the patients seems to respond to the therapy, there is a need to identify specific biomarkers that can predict a positive response, -so that patients can be stratified accordingly.

Yet, since the improved patient condition and radiological response are only transient, one might also envisage that therapies, in which compounds that interfere with the adaptation mechanism after anti-angiogenic treatment, can be combined with the anti-angiogenic therapy. Several pre-clinical studies point at a therapeutic benefit by combining bevacizumab or TKI agents with molecules that target glycolysis [145, 146] or the invasive tumor cells [147-151]. In a study from our lab (Abdul Rahim et al, manuscript in preparation), we have also found that the combination of bevacizumab with chloroquine, proposed as an autophagy inhibitor, extended survival in mice. Similar results have also been reported by another group [152].

Phase I and II clinical trials that combine bevacizumab with inhibitors of molecules involved in the adaptive response to anti-angiogenic therapy such as c-MET, PI3K, mTOR have also been initiated (NCT01113398, NCT01632228, NCT01349660, NCT02142803…). A phase II study combining bevacizumab with the mTOR inhibitor temsirolimus, for patients with recurrent GBMs after TMZ and bevacizumab, was not able to report activity of the combined therapies [153]. A pilot study combining bevacizumab with a ketogenic diet (high-fat, adequate-protein, low-carbohydrate) was also conducted but showed little efficacy [154]. Since we are here dealing with fundamental molecular processes of the cell (energetic supply, adaptation to environmental changes, cellular respiration) and given the complex network of redundant and versatile pathways that the cell can use to fulfill its energetic needs, it is likely that the key to the success of such combination therapies will strongly depend on our ability to specifically target the impaired metabolism of tumors cells, thus causing limited detrimental effects to normal cells.

In a study with bevacizumab and the EGFR inhibitor erlotinib, no difference was seen between the bevacizumab + erlotinib regimen in comparison to historical data with bevacizumab alone [27]. However, in another small study of recurrent GBM patients treated with bevacizumab, the addition of erlotinib for targeted patients that expressed EGFRvIII, significantly increased the response rate and 6-months progression free survival, highlighting the benefit of tailoring the treatment to the molecular profile of the patients' tumor [155].

4.5 Vascular normalization and drug delivery

Many clinical trials are in progress in which anti-angiogenic therapy is combined with classical chemotherapeutic agents such as the alkylating agent Temodal. In a recent study on bevacizumab naive recurrent GBM, the authors reviewed a number of completed clinical studies where bevacizumab had been given together with various chemotherapeutic agents and found that none of these studies reported improved survival compared to bevacizumab alone [156]. And the addition of bevacizumab to standard chemo- and radio-therapy regimen for the first line treatment of GBM patients (the RTOG 0825 and the AVAglio studies mentioned before) did not improve overall survival either [23, 24].

In paper II, we discussed the possibility that the reduced permeability of the tumor vasculature caused by the anti-angiogenic therapy, and the associated reduction of blood supply, might have detrimental effects on the delivery of chemotherapeutic agents to tumor cells. We proposed that the normalization of the morphology of the tumor vasculature may not necessarily lead to a normalization of its function, which would result in improved blood flow.

Others have postulated that anti-angiogenic therapies may instead induce a transient 'window of normalization' [13, 157] during which blood and oxygen supply to the tumor would be improved. A better oxygenation of the tumor may lead to an improved efficacy of radio-therapy given during this time window. This was first demonstrated in a number of pre-clinical models of subcutaneous tumors [158, 159], and later examined in the case of orthotopically implanted brain tumors [160]. Studies that attempted to deliver chemotherapeutic agents during the so-called normalization window have reported mixed results. While some reported improved efficacy [161-163], which may be related to an improved blood supply to the tumor, others reported decreased efficacy [164, 165] and attributed that to a restoration of the blood-brain-barrier.

Whether results similar to these pre-clinical results can be observed in the clinic, establishing the existence of a 'window of normalization', during which the effects of standard therapies would be improved, is being debated. In a study of 30 patients with recurrent GBMs, Sorensen et al. reported that improved blood flow, assessed by DSC-MRI, was observed in only ¼ of the patients. For this patient subpopulation, the improved blood flow was associated with a benefit in overall survival [102]. In another clinical study on newly diagnosed GBM treated with cediranib and chemoradiation, Batchelor et al. were also able to report improved perfusion and oxygenation in a subset of the patients treated with an anti-angiogenic drug. Normal angiogenesis requires a tightly regulated balance of pro- and anti-angiogenic factors [166]. The elevated levels of VEGF in pathological angiogenesis and its regulation by anti-VEGF agents might simply not be sufficient to lead to the formation of normal functioning vessels [10, 167] with improved blood flow, while restoration of the blood-brain-barrier could interfere with the biodistribution of the chemotherapeutic agents.

Several reasons may explain the difficulty of reproducing in the clinic the benefits of combined anti-angiogenic therapy with classical therapies reported in some pre-clinical studies. First, the pre-clinical models used might not reflect the heterogeneity of the clinical GBM and different phenotypes and subpopulations of GBM cells may react differently to the anti-angiogenic challenge. The subcutaneous tumor models poorly reflect what is happening in the brain, especially if, as shown in our studies, the anti-angiogenic therapies restore the integrity of the blood-brain-barrier. As discussed in Paper II and Paper III, our xenograft models of patient-derived GBMs spheroids, that reflect the angiogenic and invasive growth mechanisms of the tumor, most likely reflect the clinical features of the GBMs more closely. Then, the perfusion methodology approach used to assess blood flow may be of importance as well. DSC-MRI normally assumes the contrast agent to remain intravascular, which is typically not the case in tumors with a leaky vasculature. While leakage correction methods exist and are being used [168], DCE-MRI with multipass of contrast agent bolus may have, as discussed earlier, an advantage in that blood flow and vessel permeability are quantified separately by the model, so that the changes in these parameters induced by anti-angiogenic therapies can be evaluated independently.

In our ongoing vascular normalization study, we compare the longitudinal changes in the perfusion parameters evaluated by the different perfusion techniques in our animal models. Preliminary results have been unable to confirm the existence of a 'functional' vascular normalization window. Confirmation studies will however be needed and other GBM models should be tested as well.

5 CONCLUSIONS

Five years after its approval by the FDA for the second line treatment of GBM, bevacizumab has not lived up to its expectations. The radiological response and improved patient conditions observed in those that respond to the therapy are limited in time, and the benefit in overall survival is only marginal, whether bevacizumab is given alone or in combination with chemotherapy. Adaptation mechanisms take place, such as the activation of pro-angiogenic pathways, reflecting the versatility of the metabolic and signaling pathways that tumors cells can use to respond to changes in the environmental conditions. In this thesis, we have also shown, using a combination of imaging modalities and molecular analysis techniques, how a metabolic adaptation towards a more glycolytic metabolism can occur after anti-angiogenic therapy. This may lead to an increased acidification of the micro-environment that facilitates tumor infiltration. These findings support the idea that treatment strategies that combine bevacizumab with molecules that interfere with the adaptation mechanisms after anti-angiogenic therapy, such as glycolysis inhibitors or molecules that interfere with the invasive growth, may have a role in glioma treatment in the future. Since the mechanisms of action here is totally different from that of alkylating agents and radiotherapy, these alternative therapies could prove useful for patients who develop resistance to the standard therapies. Preclinical studies are starting to show promising results, and the success in turning these early achievements into usable clinical applications may depend on our ability to specifically target tumor cells with minimal side effects on normal cells.

As molecular and cellular therapies make their way from preclinical research to clinical studies and clinical routine, imaging strategies must evolve to properly monitor treatment effects. The strong effect of bevacizumab on the permeability of blood vessels causes drastic changes in contrast enhancement that do not reflect anti-tumor activity. MRI protocols that measure physiological and metabolic changes can definitely provide a wider picture of the changes induced by a given therapy. Experimental protocols such as Susceptibility Weighted Imaging, Restriction Spectrum Imaging, Amide Proton Transfer or Targeted Nanoparticles, to name a few, may in the future extend our ability to visualize evolving tumor features, such as the changes in vessel structure, the extent of edema, the immune response or the infiltration of tumor cells into the brain parenchyma. PET imaging, for example with proliferation, hypoxia or cellular death tracers, can complement MRI in applications where the exquisite sensitivity of this modality is beneficial, such as for the delineation of tumor borders prior to therapy, the assessment of response to therapy or the determination of the presence of infiltrated tumor cells.

GBMs are complex and heterogeneous tumors. It can therefore be expected that a successful treatment strategy will need to address the many facets of tumor development, most likely resulting in combined therapies, and relying on multi-modal imaging to provide a complete view of the tumor progression and its response to therapy.

6 FUTURE DIRECTIONS

We have discussed the potential of therapies that combine bevacizumab with molecules that interfere with the adaptation mechanisms after anti-angiogenic therapy. Molecules such as HIF1α inhibitors, glycolysis inhibitors or integrin signaling inhibitors could, for example, be good candidates, provided that they can efficiently reach their targets. Thus, issues such as specificity of the molecule to preferentially affect tumor cells, with minimal effects on normal cells, and biodistribution will need to be carefully investigated. Given the physiological changes induced by anti-angiogenic therapy on blood vessel permeability and perfusion, one strategy could be to first test the delivery of these additional compounds locally, using osmotic pumps for example, to validate the potential synergistic effect of the combined therapies, independently from issues related to the biodistribution of the compound or changes in the permeability of the blood brain barrier.

To further investigate a potential vascular normalization effect and its impact on drug delivery, we propose to perform a PET study with radiolabeled TMZ. The possibility to radiolabel TMZ and other chemotherapeutic compounds for detection by PET has been demonstrated [45, 169]. We thus plan to use this technique, together with our patient-derived xenograft models, to compare the accumulation of TMZ in the tumor tissue in vivo before and after bevacizumab treatment. From this data, we would be able to derive information about the influence of anti-angiogenic drug on the biodistribution of chemotherapeutic agents.

Several experimental techniques are being investigated for the imaging of the infiltrative compartment of tumors, since infiltrated tumor cells remain difficult to detect with the conventional imaging techniques used in the clinic today. One interesting strategy could be to combine these different protocols in an information system that would predict the degree of infiltration by comparison with reference datasets. Using our animal models with tumors showing various degrees of infiltration, the reference data could then be provided by histology.

7 REFERENCES

1. Louis, D.N., et al., *The 2007 WHO classification of tumors of the central nervous system.* Acta Neuropathol, 2007. **114**(2): p. 97-109.
2. Ohgaki, H. and P. Kleihues, *Genetic pathways to primary and secondary glioblastoma.* Am J Pathol, 2007. **170**(5): p. 1445-53.
3. Stupp, R., et al., *High-grade malignant glioma: ESMO Clinical Practice Guidelines for diagnosis, treatment and follow-up.* Ann Oncol, 2010. **21 Suppl 5**: p. v190-3.
4. Stiles, C.D., *Cancer of the central nervous system. Review of an AACR special conference in cancer research with the joint section on tumors of the AANS/CNS (San Diego, CA, June 7-11, 1997).* Biochim Biophys Acta, 1998. **1377**(1): p. R1-10.
5. Siegel, R., et al., *Cancer statistics, 2014.* CA Cancer J Clin, 2014. **64**(1): p. 9-29.
6. Stupp, R., et al., *Radiotherapy plus concomitant and adjuvant temozolomide for glioblastoma.* N Engl J Med, 2005. **352**(10): p. 987-96.
7. Stupp, R., et al., *Effects of radiotherapy with concomitant and adjuvant temozolomide versus radiotherapy alone on survival in glioblastoma in a randomised phase III study: 5-year analysis of the EORTC-NCIC trial.* Lancet Oncol, 2009. **10**(5): p. 459-66.
8. Weller, M., et al., *MGMT promoter methylation in malignant gliomas: ready for personalized medicine?* Nat Rev Neurol, 2010. **6**(1): p. 39-51.
9. Bhatia, S., et al., *The challenges posed by cancer heterogeneity.* Nat Biotechnol, 2012. **30**(7): p. 604-10.
10. Potente, M., H. Gerhardt, and P. Carmeliet, *Basic and therapeutic aspects of angiogenesis.* Cell, 2011. **146**(6): p. 873-87.
11. Baehring, J.M., *Glioblastoma multiforme--new approaches to therapy.* Cancer J, 2012. **18**(1): p. 11.
12. Folkman, J., *Angiogenesis: an organizing principle for drug discovery?* Nat Rev Drug Discov, 2007. **6**(4): p. 273-86.
13. Jain, R.K., *Normalization of tumor vasculature: an emerging concept in antiangiogenic therapy.* Science, 2005. **307**(5706): p. 58-62.
14. Calabrese, C., et al., *A perivascular niche for brain tumor stem cells.* Cancer Cell, 2007. **11**(1): p. 69-82.
15. Plate, K.H., et al., *Vascular endothelial growth factor is a potential tumor angiogenesis factor in human gliomas in vivo.* Nature, 1992. **359**(6398): p. 845-8.
16. Norden, A.D., J. Drappatz, and P.Y. Wen, *Antiangiogenic therapies for high-grade glioma.* Nat Rev Neurol, 2009. **5**(11): p. 610-20.
17. Vredenburgh, J.J., et al., *Bevacizumab plus irinotecan in recurrent glioblastoma multiforme.* J Clin Oncol, 2007. **25**(30): p. 4722-9.
18. Friedman, H.S., et al., *Bevacizumab alone and in combination with irinotecan in recurrent glioblastoma.* J Clin Oncol, 2009. **27**(28): p. 4733-40.
19. Batchelor, T.T., et al., *Phase II study of cediranib, an oral pan-vascular endothelial growth factor receptor tyrosine kinase inhibitor, in patients with recurrent glioblastoma.* J Clin Oncol, 2010. **28**(17): p. 2817-23.
20. Ahluwalia, M.S., *2010 Society for Neuro-Oncology Annual Meeting: a report of selected studies.* Expert Rev Anticancer Ther, 2011. **11**(2): p. 161-3.
21. Peak, S.J. and V.A. Levin, *Role of bevacizumab therapy in the management of glioblastoma.* Cancer Manag Res, 2010. **2**: p. 97-104.

22. Levin, V.A., et al., *Randomized double-blind placebo-controlled trial of bevacizumab therapy for radiation necrosis of the central nervous system.* Int J Radiat Oncol Biol Phys, 2011. **79**(5): p. 1487-95.
23. Gilbert, M.R., et al., *A randomized trial of bevacizumab for newly diagnosed glioblastoma.* N Engl J Med, 2014. **370**(8): p. 699-708.
24. Chinot, O.L., et al., *Bevacizumab plus radiotherapy-temozolomide for newly diagnosed glioblastoma.* N Engl J Med, 2014. **370**(8): p. 709-22.
25. Bergers, G. and D. Hanahan, *Modes of resistance to anti-angiogenic therapy.* Nat Rev Cancer, 2008. **8**(8): p. 592-603.
26. Miletic, H., et al., *Anti-VEGF therapies for malignant glioma: treatment effects and escape mechanisms.* Expert Opin Ther Targets, 2009. **13**(4): p. 455-68.
27. Sathornsumetee, S., et al., *Phase II trial of bevacizumab and erlotinib in patients with recurrent malignant glioma.* Neuro Oncol, 2010. **12**(12): p. 1300-10.
28. Lai, A., et al., *Phase II pilot study of bevacizumab in combination with temozolomide and regional radiation therapy for up-front treatment of patients with newly diagnosed glioblastoma multiforme: interim analysis of safety and tolerability.* Int J Radiat Oncol Biol Phys, 2008. **71**(5): p. 1372-80.
29. Dietrich, J., A.D. Norden, and P.Y. Wen, *Emerging antiangiogenic treatments for gliomas - efficacy and safety issues.* Curr Opin Neurol, 2008. **21**(6): p. 736-44.
30. Ranpura, V., S. Hapani, and S. Wu, *Treatment-related mortality with bevacizumab in cancer patients: a meta-analysis.* JAMA, 2011. **305**(5): p. 487-94.
31. Jenkinson, M.D., et al., *Advanced MRI in the management of adult gliomas.* Br J Neurosurg, 2007. **21**(6): p. 550-61.
32. Upadhyay, N. and A.D. Waldman, *Conventional MRI evaluation of gliomas.* Br J Radiol, 2011. **84 Spec No 2**: p. S107-11.
33. Nihashi, T., I.J. Dahabreh, and T. Terasawa, *PET in the clinical management of glioma: evidence map.* AJR Am J Roentgenol, 2013. **200**(6): p. W654-60.
34. Jain, R., *Perfusion CT imaging of brain tumors: an overview.* AJNR Am J Neuroradiol, 2011. **32**(9): p. 1570-7.
35. Samnick, S., et al., *Clinical value of iodine-123-alpha-methyl-L-tyrosine single-photon emission tomography in the differential diagnosis of recurrent brain tumor in patients pretreated for glioma at follow-up.* J Clin Oncol, 2002. **20**(2): p. 396-404.
36. Harwood-Nash, D.C., *Neuroimaging and pediatrics.* Curr Opin Neurol Neurosurg, 1991. **4**(6): p. 858-63.
37. Unsgard, G., et al., *Intra-operative imaging with 3D ultrasound in neurosurgery.* Acta Neurochir Suppl, 2011. **109**: p. 181-6.
38. Law, M., et al., *Glioma grading: sensitivity, specificity, and predictive values of perfusion MR imaging and proton MR spectroscopic imaging compared with conventional MR imaging.* AJNR Am J Neuroradiol, 2003. **24**(10): p. 1989-98.
39. Hu, L.S., et al., *Relative cerebral blood volume values to differentiate high-grade glioma recurrence from posttreatment radiation effect: direct correlation between image-guided tissue histopathology and localized dynamic susceptibility-weighted contrast-enhanced perfusion MR imaging measurements.* AJNR Am J Neuroradiol, 2009. **30**(3): p. 552-8.
40. Moller-Hartmann, W., et al., *Clinical application of proton magnetic resonance spectroscopy in the diagnosis of intracranial mass lesions.* Neuroradiology, 2002. **44**(5): p. 371-81.
41. Rock, J.P., et al., *Correlations between magnetic resonance spectroscopy and image-guided histopathology, with special attention to radiation necrosis.* Neurosurgery, 2002. **51**(4): p. 912-9; discussion 919-20.

42. Gulyas, B. and C. Halldin, *New PET radiopharmaceuticals beyond FDG for brain tumor imaging.* Q J Nucl Med Mol Imaging, 2012. **56**(2): p. 173-90.
43. Blankenberg, F.G., *In vivo detection of apoptosis.* J Nucl Med, 2008. **49 Suppl 2**: p. 81S-95S.
44. Mendichovszky, I. and A. Jackson, *Imaging hypoxia in gliomas.* Br J Radiol, 2011. **84 Spec No 2**: p. S145-58.
45. Rosso, L., et al., *A new model for prediction of drug distribution in tumor and normal tissues: pharmacokinetics of temozolomide in glioma patients.* Cancer Res, 2009. **69**(1): p. 120-7.
46. Pirotte, B., et al., *Comparison of 18F-FDG and 11C-methionine for PET-guided stereotactic brain biopsy of gliomas.* J Nucl Med, 2004. **45**(8): p. 1293-8.
47. Hutterer, M., et al., *O-(2-18F-fluoroethyl)-L-tyrosine PET predicts failure of antiangiogenic treatment in patients with recurrent high-grade glioma.* J Nucl Med, 2011. **52**(6): p. 856-64.
48. Idema, A.J., et al., *3'-Deoxy-3'-18F-fluorothymidine PET-derived proliferative volume predicts overall survival in high-grade glioma patients.* J Nucl Med, 2012. **53**(12): p. 1904-10.
49. Bruehlmeier, M., et al., *Assessment of hypoxia and perfusion in human brain tumors using PET with 18F-fluoromisonidazole and 15O-H2O.* J Nucl Med, 2004. **45**(11): p. 1851-9.
50. Macdonald, D.R., et al., *Response criteria for phase II studies of supratentorial malignant glioma.* J Clin Oncol, 1990. **8**(7): p. 1277-80.
51. Brandsma, D., et al., *Clinical features, mechanisms, and management of pseudoprogression in malignant gliomas.* Lancet Oncol, 2008. **9**(5): p. 453-61.
52. Hein, P.A., et al., *Diffusion-weighted imaging in the follow-up of treated high-grade gliomas: tumor recurrence versus radiation injury.* AJNR Am J Neuroradiol, 2004. **25**(2): p. 201-9.
53. Glaudemans, A.W., et al., *Value of 11C-methionine PET in imaging brain tumors and metastases.* Eur J Nucl Med Mol Imaging, 2013. **40**(4): p. 615-35.
54. Singhal, T., et al., *11C-L-methionine positron emission tomography in the clinical management of cerebral gliomas.* Mol Imaging Biol, 2008. **10**(1): p. 1-18.
55. Alkonyi, B., et al., *Accurate differentiation of recurrent gliomas from radiation injury by kinetic analysis of alpha-11C-methyl-L-tryptophan PET.* J Nucl Med, 2012. **53**(7): p. 1058-64.
56. Hygino da Cruz, L.C., Jr., et al., *Pseudoprogression and pseudoresponse: imaging challenges in the assessment of posttreatment glioma.* AJNR Am J Neuroradiol, 2011. **32**(11): p. 1978-85.
57. Lutz, K., et al., *Neuroradiological response criteria for high-grade gliomas.* Clin Neuroradiol, 2011. **21**(4): p. 199-205.
58. Huszthy, P.C., et al., *In vivo models of primary brain tumors: pitfalls and perspectives.* Neuro Oncol, 2012. **14**(8): p. 979-93.
59. Li, A., et al., *Genomic changes and gene expression profiles reveal that established glioma cell lines are poorly representative of primary human gliomas.* Mol Cancer Res, 2008. **6**(1): p. 21-30.
60. Sakariassen, P.O., et al., *Angiogenesis-independent tumor growth mediated by stem-like cancer cells.* Proc Natl Acad Sci U S A, 2006. **103**(44): p. 16466-71.
61. Wang, J., et al., *A reproducible brain tumor model established from human glioblastoma biopsies.* BMC Cancer, 2009. **9**: p. 465.
62. Koh, T.S., et al., *The inclusion of capillary distribution in the adiabatic tissue homogeneity model of blood flow.* Phys Med Biol, 2001. **46**(5): p. 1519-38.
63. Tofts, P.S., et al., *Estimating kinetic parameters from dynamic contrast-enhanced T(1)-weighted MRI of a diffusable tracer: standardized quantities and symbols.* J Magn Reson Imaging, 1999. **10**(3): p. 223-32.
64. Taxt, T., et al., *Single-channel blind estimation of arterial input function and tissue impulse response in DCE-MRI.* IEEE Trans Biomed Eng, 2012. **59**(4): p. 1012-21.

65. Bartoš, M., et al., *Perfusion Analysis of Dynamic Contrast Enhanced Magnetic Resonance Images Using a Fully Continuous Tissue Homogeneity Model with Mean Transit Time Dispersion and Frequency Domain Estimation of the Signal Delay.* Anal Biomed Sign Images, 2010. **20**: p. 269-274.
66. Young, H., et al., *Measurement of clinical and subclinical tumor response using [18F]-fluorodeoxyglucose and positron emission tomography: review and 1999 EORTC recommendations. European Organization for Research and Treatment of Cancer (EORTC) PET Study Group.* Eur J Cancer, 1999. **35**(13): p. 1773-82.
67. Wong, E.T., et al., *Bevacizumab for recurrent glioblastoma multiforme: a meta-analysis.* J Natl Compr Canc Netw, 2011. **9**(4): p. 403-7.
68. Shen, G., et al., *Hypoxia-regulated microRNAs in human cancer.* Acta Pharmacol Sin, 2013. **34**(3): p. 336-41.
69. Howe, F.A., et al., *Metabolic profiles of human brain tumors using quantitative in vivo 1H magnetic resonance spectroscopy.* Magn Reson Med, 2003. **49**(2): p. 223-32.
70. Gatenby, R.A., et al., *Acid-mediated tumor invasion: a multidisciplinary study.* Cancer Res, 2006. **66**(10): p. 5216-23.
71. Gauvain, K.M., et al., *Evaluating pediatric brain tumor cellularity with diffusion-tensor imaging.* AJR Am J Roentgenol, 2001. **177**(2): p. 449-54.
72. Ellingson, B.M., et al., *Validation of functional diffusion maps (fDMs) as a biomarker for human glioma cellularity.* J Magn Reson Imaging, 2010. **31**(3): p. 538-48.
73. Gerstner, E.R., M.P. Frosch, and T.T. Batchelor, *Diffusion magnetic resonance imaging detects pathologically confirmed, nonenhancing tumor progression in a patient with recurrent glioblastoma receiving bevacizumab.* J Clin Oncol, 2010. **28**(6): p. e91-3.
74. Gilbert, M.R., *RTOG 0825: Phase III double-blind placebo-controlled trial evaluating bevacizumab (Bev) in patients (Pts) with newly diagnosed glioblastoma (GBM).* J Clin Oncol, 2013. **31**(18).
75. Rosenstein, J.M. and J.M. Krum, *New roles for VEGF in nervous tissue--beyond blood vessels.* Exp Neurol, 2004. **187**(2): p. 246-53.
76. Jin, K.L., X.O. Mao, and D.A. Greenberg, *Vascular endothelial growth factor: direct neuroprotective effect in in vitro ischemia.* Proc Natl Acad Sci U S A, 2000. **97**(18): p. 10242-7.
77. Svensson, B., et al., *Vascular endothelial growth factor protects cultured rat hippocampal neurons against hypoxic injury via an antiexcitotoxic, caspase-independent mechanism.* J Cereb Blood Flow Metab, 2002. **22**(10): p. 1170-5.
78. Ma, Y., et al., *VEGF protects rat cortical neurons from mechanical trauma injury induced apoptosis via the MEK/ERK pathway.* Brain Res Bull, 2011. **86**(5-6): p. 441-6.
79. Licht, T., et al., *Reversible modulations of neuronal plasticity by VEGF.* Proc Natl Acad Sci U S A, 2011. **108**(12): p. 5081-6.
80. Therasse, P., et al., *New guidelines to evaluate the response to treatment in solid tumors. European Organization for Research and Treatment of Cancer, National Cancer Institute of the United States, National Cancer Institute of Canada.* J Natl Cancer Inst, 2000. **92**(3): p. 205-16.
81. Nagpal, S., G. Harsh, and L. Recht, *Bevacizumab improves quality of life in patients with recurrent glioblastoma.* Chemother Res Pract, 2011. **2011**: p. 602812.
82. Arbab, A.S., *Activation of alternative pathways of angiogenesis and involvement of stem cells following anti-angiogenesis treatment in glioma.* Histol Histopathol, 2012. **27**(5): p. 549-57.
83. Wick, W., et al., *Patterns of progression in malignant glioma following anti-VEGF therapy: perceptions and evidence.* Curr Neurol Neurosci Rep, 2011. **11**(3): p. 305-12.
84. Lu, K.V. and G. Bergers, *Mechanisms of evasive resistance to anti-VEGF therapy in glioblastoma.* CNS Oncol, 2013. **2**(1): p. 49-65.
85. Verhoeff, J.J., et al., *Concerns about anti-angiogenic treatment in patients with glioblastoma multiforme.* BMC Cancer, 2009. **9**: p. 444.

86. Holdhoff, M. and S.A. Grossman, *Controversies in the adjuvant therapy of high-grade gliomas.* Oncologist, 2011. **16**(3): p. 351-8.
87. Rinne, M.L., et al., *Update on bevacizumab and other angiogenesis inhibitors for brain cancer.* Expert Opin Emerg Drugs, 2013. **18**(2): p. 137-53.
88. Norden, A.D., et al., *An exploratory survival analysis of anti-angiogenic therapy for recurrent malignant glioma.* J Neurooncol, 2009. **92**(2): p. 149-55.
89. Wick, W., et al., *Bevacizumab and recurrent malignant gliomas: a European perspective.* J Clin Oncol, 2010. **28**(12): p. e188-9; author reply e190-2.
90. Huang, H., et al., *An updated meta-analysis of fatal adverse events caused by bevacizumab therapy in cancer patients.* PLoS One, 2014. **9**(3): p. e89960.
91. Schutz, F.A., et al., *Bevacizumab increases the risk of arterial ischemia: a large study in cancer patients with a focus on different subgroup outcomes.* Ann Oncol, 2011. **22**(6): p. 1404-12.
92. Chen, X.L., et al., *Angiogenesis inhibitor bevacizumab increases the risk of ischemic heart disease associated with chemotherapy: a meta-analysis.* PLoS One, 2013. **8**(6): p. e66721.
93. Hapani, S., et al., *Increased risk of serious hemorrhage with bevacizumab in cancer patients: a meta-analysis.* Oncology, 2010. **79**(1-2): p. 27-38.
94. Weller, M. and W.K. Yung, *Angiogenesis inhibition for glioblastoma at the edge: beyond AVAGlio and RTOG 0825.* Neuro Oncol, 2013. **15**(8): p. 971.
95. Stupp, R. and M. Weller, *Questions regarding the optimal use of bevacizumab in glioblastoma: a moving target.* Neuro Oncol, 2014.
96. Pope, W.B., J.R. Young, and B.M. Ellingson, *Advances in MRI assessment of gliomas and response to anti-VEGF therapy.* Curr Neurol Neurosci Rep, 2011. **11**(3): p. 336-44.
97. Norden, A.D., J. Drappatz, and P.Y. Wen, *Novel anti-angiogenic therapies for malignant gliomas.* Lancet Neurol, 2008. **7**(12): p. 1152-60.
98. de Groot, J.F., et al., *Tumor invasion after treatment of glioblastoma with bevacizumab: radiographic and pathologic correlation in humans and mice.* Neuro Oncol, 2010. **12**(3): p. 233-42.
99. Narayana, A., et al., *Change in pattern of relapse after antiangiogenic therapy in high-grade glioma.* Int J Radiat Oncol Biol Phys, 2012. **82**(1): p. 77-82.
100. van den Bent, M.J., et al., *End point assessment in gliomas: novel treatments limit usefulness of classical Macdonald's Criteria.* J Clin Oncol, 2009. **27**(18): p. 2905-8.
101. Wen, P.Y., et al., *Updated response assessment criteria for high-grade gliomas: response assessment in neuro-oncology working group.* J Clin Oncol, 2010. **28**(11): p. 1963-72.
102. Sorensen, A.G., et al., *Increased survival of glioblastoma patients who respond to antiangiogenic therapy with elevated blood perfusion.* Cancer Res, 2012. **72**(2): p. 402-7.
103. Cha, S., et al., *Dynamic contrast-enhanced T2-weighted MR imaging of recurrent malignant gliomas treated with thalidomide and carboplatin.* AJNR Am J Neuroradiol, 2000. **21**(5): p. 881-90.
104. Aquino, D., et al., *Parametric response maps of perfusion MRI may identify recurrent glioblastomas responsive to bevacizumab and irinotecan.* PLoS One, 2014. **9**(3): p. e90535.
105. Galban, C.J., et al., *Prospective analysis of parametric response map-derived MRI biomarkers: identification of early and distinct glioma response patterns not predicted by standard radiographic assessment.* Clin Cancer Res, 2011. **17**(14): p. 4751-60.
106. Moffat, B.A., et al., *Functional diffusion map: a noninvasive MRI biomarker for early stratification of clinical brain tumor response.* Proc Natl Acad Sci U S A, 2005. **102**(15): p. 5524-9.
107. Hamstra, D.A., et al., *Evaluation of the functional diffusion map as an early biomarker of time-to-progression and overall survival in high-grade glioma.* Proc Natl Acad Sci U S A, 2005. **102**(46): p. 16759-64.

108. Aronen, H.J., et al., *Cerebral blood volume maps of gliomas: comparison with tumor grade and histologic findings.* Radiology, 1994. **191**(1): p. 41-51.
109. Gossmann, A., et al., *Dynamic contrast-enhanced magnetic resonance imaging as a surrogate marker of tumor response to anti-angiogenic therapy in a xenograft model of glioblastoma multiforme.* J Magn Reson Imaging, 2002. **15**(3): p. 233-40.
110. Larsson, H.B., et al., *Measurement of brain perfusion, blood volume, and blood-brain barrier permeability, using dynamic contrast-enhanced T(1)-weighted MRI at 3 tesla.* Magn Reson Med, 2009. **62**(5): p. 1270-81.
111. Larsen, V.A., et al., *Evaluation of dynamic contrast-enhanced T1-weighted perfusion MRI in the differentiation of tumor recurrence from radiation necrosis.* Neuroradiology, 2013. **55**(3): p. 361-9.
112. Taylor, J.S. and W.E. Reddick, *Evolution from empirical dynamic contrast-enhanced magnetic resonance imaging to pharmacokinetic MRI.* Adv Drug Deliv Rev, 2000. **41**(1): p. 91-110.
113. Leach, M.O., et al., *The assessment of antiangiogenic and antivascular therapies in early-stage clinical trials using magnetic resonance imaging: issues and recommendations.* Br J Cancer, 2005. **92**(9): p. 1599-610.
114. Barbier, E.L., et al., *A model of the dual effect of gadopentetate dimeglumine on dynamic brain MR images.* J Magn Reson Imaging, 1999. **10**(3): p. 242-53.
115. Kim, E.J., et al., *Simultaneous acquisition of perfusion and permeability from corrected relaxation rates with dynamic susceptibility contrast dual gradient echo.* Magn Reson Imaging, 2004. **22**(3): p. 307-14.
116. Pope, W.B., et al., *Apparent diffusion coefficient histogram analysis stratifies progression-free and overall survival in patients with recurrent GBM treated with bevacizumab: a multi-center study.* J Neurooncol, 2012. **108**(3): p. 491-8.
117. Kothari, P.D., et al., *Longitudinal restriction spectrum imaging is resistant to pseudoresponse in patients with high-grade gliomas treated with bevacizumab.* AJNR Am J Neuroradiol, 2013. **34**(9): p. 1752-7.
118. Grabner, G., et al., *Longitudinal brain imaging of five malignant glioma patients treated with bevacizumab using susceptibility-weighted magnetic resonance imaging at 7 T.* Magn Reson Imaging, 2012. **30**(1): p. 139-47.
119. Mohammed, W., et al., *Clinical applications of susceptibility-weighted imaging in detecting and grading intracranial gliomas: a review.* Cancer Imaging, 2013. **13**: p. 186-95.
120. Lupo, J.M., et al., *Using susceptibility-weighted imaging to determine response to combined anti-angiogenic, cytotoxic, and radiation therapy in patients with glioblastoma multiforme.* Neuro Oncol, 2013. **15**(4): p. 480-9.
121. Robinson, S.P., et al., *Magnetic resonance imaging techniques for monitoring changes in tumor oxygenation and blood flow.* Semin Radiat Oncol, 1998. **8**(3): p. 197-207.
122. Taylor, N.J., et al., *BOLD MRI of human tumor oxygenation during carbogen breathing.* J Magn Reson Imaging, 2001. **14**(2): p. 156-63.
123. Ben Bashat, D., et al., *Hemodynamic response imaging: a potential tool for the assessment of angiogenesis in brain tumors.* PLoS One, 2012. **7**(11): p. e49416.
124. McLean, M.A., et al., *Repeatability of edited lactate and other metabolites in astrocytoma at 3T.* J Magn Reson Imaging, 2012. **36**(2): p. 468-75.
125. Andronesi, O.C., et al., *Detection of 2-hydroxyglutarate in IDH-mutated glioma patients by in vivo spectral-editing and 2D correlation magnetic resonance spectroscopy.* Sci Transl Med, 2012. **4**(116): p. 116ra4.

126. Ratai, E.M., et al., *Magnetic resonance spectroscopy as an early indicator of response to anti-angiogenic therapy in patients with recurrent glioblastoma: RTOG 0625/ACRIN 6677.* Neuro Oncol, 2013. **15**(7): p. 936-44.
127. Hattingen, E., et al., *Phospholipid metabolites in recurrent glioblastoma: in vivo markers detect different tumor phenotypes before and under antiangiogenic therapy.* PLoS One, 2013. **8**(3): p. e56439.
128. Bohndiek, S.E., et al., *Detection of tumor response to a vascular disrupting agent by hyperpolarized 13C magnetic resonance spectroscopy.* Mol Cancer Ther, 2010. **9**(12): p. 3278-88.
129. Harris, R.J., et al., *Pre- and post-contrast three-dimensional double inversion-recovery MRI in human glioblastoma.* J Neurooncol, 2013. **112**(2): p. 257-66.
130. Galldiks, N., et al., *Earlier diagnosis of progressive disease during bevacizumab treatment using O-(2-18F-fluorethyl)-L-tyrosine positron emission tomography in comparison with magnetic resonance imaging.* Mol Imaging, 2013. **12**(5): p. 273-6.
131. Norden, A.D., et al., *Bevacizumab for recurrent malignant gliomas: efficacy, toxicity, and patterns of recurrence.* Neurology, 2008. **70**(10): p. 779-87.
132. Bloch, O., et al., *Disseminated progression of glioblastoma after treatment with bevacizumab.* Clin Neurol Neurosurg, 2013. **115**(9): p. 1795-801.
133. Ebos, J.M. and R.S. Kerbel, *Antiangiogenic therapy: impact on invasion, disease progression, and metastasis.* Nat Rev Clin Oncol, 2011. **8**(4): p. 210-21.
134. Ellingson, B.M., et al., *Volumetric analysis of functional diffusion maps is a predictive imaging biomarker for cytotoxic and anti-angiogenic treatments in malignant gliomas.* J Neurooncol, 2011. **102**(1): p. 95-103.
135. Pope, W.B., et al., *Recurrent glioblastoma multiforme: ADC histogram analysis predicts response to bevacizumab treatment.* Radiology, 2009. **252**(1): p. 182-9.
136. Colvin, D.C., et al., *Earlier detection of tumor treatment response using magnetic resonance diffusion imaging with oscillating gradients.* Magn Reson Imaging, 2011. **29**(3): p. 315-23.
137. Zhou, J., et al., *Amide proton transfer (APT) contrast for imaging of brain tumors.* Magn Reson Med, 2003. **50**(6): p. 1120-6.
138. Zhou, J., et al., *Three-dimensional amide proton transfer MR imaging of gliomas: Initial experience and comparison with gadolinium enhancement.* J Magn Reson Imaging, 2013. **38**(5): p. 1119-28.
139. Sagiyama, K., et al., *In vivo chemical exchange saturation transfer imaging allows early detection of a therapeutic response in glioblastoma.* Proc Natl Acad Sci U S A, 2014. **111**(12): p. 4542-7.
140. Zhou, J., et al., *Differentiation between glioma and radiation necrosis using molecular magnetic resonance imaging of endogenous proteins and peptides.* Nat Med, 2011. **17**(1): p. 130-4.
141. Kracht, L.W., et al., *Delineation of brain tumor extent with [11C]L-methionine positron emission tomography: local comparison with stereotactic histopathology.* Clin Cancer Res, 2004. **10**(21): p. 7163-70.
142. Kinoshita, M., et al., *A novel PET index, 18F-FDG-11C-methionine uptake decoupling score, reflects glioma cell infiltration.* J Nucl Med, 2012. **53**(11): p. 1701-8.
143. Scaringi, C., et al., *Integrin inhibitor cilengitide for the treatment of glioblastoma: a brief overview of current clinical results.* Anticancer Res, 2012. **32**(10): p. 4213-23.
144. de Groot, J.F., et al., *Phase II study of aflibercept in recurrent malignant glioma: a North American Brain Tumor Consortium study.* J Clin Oncol, 2011. **29**(19): p. 2689-95.
145. Kumar, K., et al., *Dichloroacetate reverses the hypoxic adaptation to bevacizumab and enhances its antitumor effects in mouse xenografts.* J Mol Med (Berl), 2013. **91**(6): p. 749-58.
146. McIntyre, A., et al., *Carbonic anhydrase IX promotes tumor growth and necrosis in vivo and inhibition enhances anti-VEGF therapy.* Clin Cancer Res, 2012. **18**(11): p. 3100-11.

147. Navis, A.C., et al., *Effects of dual targeting of tumor cells and stroma in human glioblastoma xenografts with a tyrosine kinase inhibitor against c-MET and VEGFR2.* PLoS One, 2013. **8**(3): p. e58262.
148. Huveldt, D., et al., *Targeting Src family kinases inhibits bevacizumab-induced glioma cell invasion.* PLoS One, 2013. **8**(2): p. e56505.
149. Jahangiri, A., et al., *Gene expression profile identifies tyrosine kinase c-Met as a targetable mediator of antiangiogenic therapy resistance.* Clin Cancer Res, 2013. **19**(7): p. 1773-83.
150. Lu, K.V., et al., *VEGF inhibits tumor cell invasion and mesenchymal transition through a MET/VEGFR2 complex.* Cancer Cell, 2012. **22**(1): p. 21-35.
151. Carbonell, W.S., et al., *beta1 integrin targeting potentiates antiangiogenic therapy and inhibits the growth of bevacizumab-resistant glioblastoma.* Cancer Res, 2013. **73**(10): p. 3145-54.
152. Hu, Y.L., et al., *Hypoxia-induced autophagy promotes tumor cell survival and adaptation to antiangiogenic treatment in glioblastoma.* Cancer Res, 2012. **72**(7): p. 1773-83.
153. Lassen, U., et al., *Phase II study of bevacizumab and temsirolimus combination therapy for recurrent glioblastoma multiforme.* Anticancer Res, 2013. **33**(4): p. 1657-60.
154. Rieger, J., et al., *ERGO: a pilot study of ketogenic diet in recurrent glioblastoma.* Int J Oncol, 2014. **44**(6): p. 1843-52.
155. D'Alessandris, Q.G., et al., *Targeted therapy with bevacizumab and erlotinib tailored to the molecular profile of patients with recurrent glioblastoma. Preliminary experience.* Acta Neurochir (Wien), 2013. **155**(1): p. 33-40.
156. Reardon, D.A., et al., *Phase II study of carboplatin, irinotecan, and bevacizumab for bevacizumab naive, recurrent glioblastoma.* J Neurooncol, 2012. **107**(1): p. 155-64.
157. Carmeliet, P. and R.K. Jain, *Principles and mechanisms of vessel normalization for cancer and other angiogenic diseases.* Nat Rev Drug Discov, 2011. **10**(6): p. 417-27.
158. Ma, J., et al., *Pharmacodynamic-mediated effects of the angiogenesis inhibitor SU5416 on the tumor disposition of temozolomide in subcutaneous and intracerebral glioma xenograft models.* J Pharmacol Exp Ther, 2003. **305**(3): p. 833-9.
159. Tong, R.T., et al., *Vascular normalization by vascular endothelial growth factor receptor 2 blockade induces a pressure gradient across the vasculature and improves drug penetration in tumors.* Cancer Res, 2004. **64**(11): p. 3731-6.
160. Winkler, F., et al., *Kinetics of vascular normalization by VEGFR2 blockade governs brain tumor response to radiation: role of oxygenation, angiopoietin-1, and matrix metalloproteinases.* Cancer Cell, 2004. **6**(6): p. 553-63.
161. Son, M.J., et al., *Combination treatment with temozolomide and thalidomide inhibits tumor growth and angiogenesis in an orthotopic glioma model.* Int J Oncol, 2006. **28**(1): p. 53-9.
162. Mathieu, V., et al., *Combining bevacizumab with temozolomide increases the antitumor efficacy of temozolomide in a human glioblastoma orthotopic xenograft model.* Neoplasia, 2008. **10**(12): p. 1383-92.
163. Zhou, Q. and J.M. Gallo, *Differential effect of sunitinib on the distribution of temozolomide in an orthotopic glioma model.* Neuro Oncol, 2009. **11**(3): p. 301-10.
164. Ma, J., et al., *Pharmacodynamic-mediated reduction of temozolomide tumor concentrations by the angiogenesis inhibitor TNP-470.* Cancer Res, 2001. **61**(14): p. 5491-8.
165. Claes, A., et al., *Antiangiogenic compounds interfere with chemotherapy of brain tumors due to vessel normalization.* Mol Cancer Ther, 2008. **7**(1): p. 71-8.
166. Batchelor, T.T., et al., *Improved tumor oxygenation and survival in glioblastoma patients who show increased blood perfusion after cediranib and chemoradiation.* Proc Natl Acad Sci U S A, 2013. **110**(47): p. 19059-64.

167. Noonan, D.M., et al., *Inflammation, inflammatory cells and angiogenesis: decisions and indecisions.* Cancer Metastasis Rev, 2008. **27**(1): p. 31-40.
168. Hu, L.S., et al., *Optimized preload leakage-correction methods to improve the diagnostic accuracy of dynamic susceptibility-weighted contrast-enhanced perfusion MR imaging in posttreatment gliomas.* AJNR Am J Neuroradiol, 2010. **31**(1): p. 40-8.
169. Van der Veldt, A.A., et al., *Rapid decrease in delivery of chemotherapy to tumors after anti-VEGF therapy: implications for scheduling of anti-angiogenic drugs.* Cancer Cell, 2012. **21**(1): p. 82-91.